Title

Rapid and precise engineering of the Caenorhabditis elegans genome with lethal mutation co-conversion and inactivation of NHEJ repair.

Journal

Genetics, 199(2)

ISSN

0016-6731

Author

Ward, Jordan D

Publication Date

2015-02-01

DOI

10.1534/genetics.114.172361

Peer reviewed

Rapid and Precise Engineering of the *Caenorhabditis elegans* Genome with Lethal Mutation Co-Conversion and Inactivation of NHEJ Repair

Jordan D. Ward
Department of Cellular and Molecular Pharmacology, University of California, San Francisco, California 94158
ORCID ID: 0000-0001-9870-8936 (J.D.W.)

ABSTRACT As in other organisms, CRISPR/Cas9 methods provide a powerful approach for genome editing in the nematode *Caenorhabditis elegans*. Oligonucleotides are excellent repair templates for introducing substitutions and short insertions, as they are cost effective, require no cloning, and appear in other organisms to target changes by homologous recombination at DNA double-strand breaks (DSBs). Here, I describe a methodology in *C. elegans* to efficiently knock in epitope tags in 8–9 days, using a temperature-sensitive lethal mutation in the *pha-1* gene as a co-conversion marker. I demonstrate that 60mer oligos with 29 bp of homology drive efficient knock-in of point mutations, and that disabling nonhomologous end joining by RNAi inactivation of the *cku-80* gene significantly improves knock-in efficiency. Homology arms of 35–80 bp are sufficient for efficient editing and DSBs up to 54 bp away from the insertion site produced knock-ins. These findings will likely be applicable for a range of genome editing approaches in *C. elegans*, which will improve editing efficiency and minimize screening efforts.

KEYWORDS oligonucleotide-mediated homologous recombination; CRISPR/Cas9; nonhomologous end joining; *pha-1*; co-conversion

SEQUENCE-SPECIFIC nucleases are a critical tool for manipulation of DNA sequences. The bacterial type II clustered regularly interspaced short palindromic repeats (CRISPR) system, which normally protects against viral DNA and provides a memory of exposure (Jinek *et al.* 2012), has recently revolutionized genome editing in multiple organisms (Cong *et al.* 2013; DiCarlo *et al.* 2013; Gratz *et al.* 2013; Hwang *et al.* 2013; Li *et al.* 2013; Ran *et al.* 2013; Gratz *et al.* 2014; Nakanishi *et al.* 2014). For genome editing, the system has been simplified to two components: the Cas9 nuclease, which generates DNA double-strand breaks (DSBs), and a chimeric small guide RNA (sgRNA) that fills the function of two small RNAs in the native bacterial system (Cong *et al.* 2013). Specific genomic sequences are targeted by the 5′-most 15–20 bp of the sgRNA through the formation of an RNA:DNA hybrid (Jinek *et al.* 2012; Mali *et al.* 2013). An NGG motif (protospacer adjacent motif, PAM) must immediately follow the target sequence in the genome (Jinek *et al.* 2012; Ran *et al.* 2013). This PAM directs Cas9 to cleave the DNA 3 bp 5′ to the PAM (Jinek *et al.* 2012). Depending on the desired experimental outcome, one can select for error-prone repair by pathways such as nonhomologous end joining (NHEJ) to generate insertion–deletion (indel) mutations, or homologous recombination to knock in specific sequences.

Initial genome editing methods in *Caenorhabditis elegans* harnessed excision of a Tc or Mos transposon to generate a DSB, and a plasmid repair template to knock in (Plasterk and Groenen 1992; Robert and Bessereau 2007; Frøkjaer-Jensen *et al.* 2008; Frøkjær-Jensen *et al.* 2012), or delete (Frøkjær-Jensen *et al.* 2010) desired sequences through homologous recombination. These methods are robust, but the relative rarity of the editing event requires use of a selectable marker, such as *unc-119* rescue or antibiotic resistance (Frøkjaer-Jensen *et al.* 2008; Giordano-Santini *et al.* 2010), and a transposon site is ideally needed within 1–2 kb of the desired edit (Robert and Bessereau 2007). Zinc finger and transcription activator-like effector nucleases (Wood *et al.* 2011) and CRISPR/Cas9 have allowed for similar efficient editing without the constraint of transposon insertions. In particular, the ease and rapidity of generating new sgRNAs for the CRISPR/Cas9 system means that transgenic strains can be created precisely and rapidly and any endogenous

doi: 10.1534/genetics.114.172361
Manuscript received November 3, 2014; accepted for publication December 8, 2014; published Early Online December 9, 2014.
Available freely online through the author-supported open access option.
Supporting information is available online at http://www.genetics.org/lookup/suppl/doi:10.1534/genetics.114.172361/-/DC1.
Address for correspondence: University of California, San Francisco, Mission Bay, Genentech Hall S574, 600 16th St., San Francisco, CA 94158.
E-mail: jordan.ward@ucsf.edu

NGG sequence can theoretically be targeted. Several CRISPR/Cas9 systems have been described, each with individual strengths and weaknesses (Waaijers and Boxem 2014). Cas9 can be delivered by micro-injection of *in vitro* transcribed mRNA (Chiu *et al.* 2013; Lo *et al.* 2013), pure protein (Cho *et al.* 2013), or plasmid DNA (Chen *et al.* 2013b; Dickinson *et al.* 2013; Friedland *et al.* 2013; Katic and Grosshans 2013; Waaijers *et al.* 2013). Similarly, the sgRNAs can be introduced by *in vitro* transcription, which does not require polyA tailing or 5′ methyl cap addition (Chiu *et al.* 2013; Cho *et al.* 2013; Lo *et al.* 2013), or driven by RNA polymerase III promoters such as U6 (Chen *et al.* 2013b; Dickinson *et al.* 2013; Friedland *et al.* 2013; Katic and Grosshans 2013; Waaijers *et al.* 2013) or *rpr-1* (Chiu *et al.* 2013). Most groups use the chimeric sgRNA, though a previous report described higher *in vitro* nuclease activity using the two separate bacterial small RNAs (Lo *et al.* 2013). Multiple groups have developed protocols for both knockouts and knock-ins. Knock-ins have been primarily generated through efficient selection schemes based on the earlier MosI-mediated single-copy transgene insertion methods using genetic markers such as *unc-119* (Dickinson *et al.* 2013), drug resistance markers (Chen *et al.* 2013b), or fluorescence (Tzur *et al.* 2013). Typically, plasmid repair templates with 1 kb or more of homology flanking the insert have been used (Chen *et al.* 2013b; Dickinson *et al.* 2013; Tzur *et al.* 2013; Kim *et al.* 2014).

Recently, several reports have described methods to introduce single-basepair changes, small epitopes, and larger tags such as GFP without the need for selectable markers; these approaches either directly screened all F_1 progeny from co-injection marker positive animals (Paix *et al.* 2014) or employed a co-CRISPR/co-conversion approach where selection for one editing event resulted in an enrichment for edits at unrelated loci (Arribere *et al.* 2014; Kim *et al.* 2014). Direct screening of F_1's allows editing without introduction of additional mutations, but is more labor intensive, while co-CRISPR/co-conversion allows for identification of editing events while minimizing hands-on screening, but requires outcrossing or meiotic segregation of the marker allele. Co-CRISPR selects for mutation in *the unc*-22 gene, with mutant homozygotes identified in the F_2 progeny of co-injection marker positive animals, or less frequently in the F_1 progeny (Kim *et al.* 2014), though haploinsufficiency of the *unc-22* locus in 1% nicotine should allow for identification of *unc-22* mutant heterozygotes in F_1 animals (Moerman and Baillie 1979). Co-conversion selects for knock-in of dominant alleles in the *dpy-10*, *sqt-1*, or *rol-6* genes in the F_1 progeny of injected animals (Arribere *et al.* 2014).

The goal of this study was to test whether repair of a temperature-sensitive lethal point mutation could be used as an alternate co-conversion marker, as such an approach could in theory provide robust selection, minimal screening, and no requirement for outcrossing or meiotic segregation of marker alleles/mutations. I focused on using single-stranded oligonucleotides (oligos) as a template as they have been successfully used in a range of model organisms (Igoucheva *et al.* 2001; Storici *et al.* 2003; Chen *et al.* 2011; Bedell *et al.* 2012; DiCarlo *et al.* 2013), are cost effective, and require no cloning. In *C. elegans*, oligonucleotides have been used to introduce single-base changes (Arribere *et al.* 2014; Zhao *et al.* 2014), inactivate genes by introducing premature stop codons or deleting sequences (Lo *et al.* 2013; Paix *et al.* 2014), or insert small protein epitopes (Lo *et al.* 2013; Paix *et al.* 2014). Introduction of epitopes seamlessly into endogenous loci has numerous experimental uses: chromatin immunoprecipitation, purification of protein complexes followed by mass spectrometry, and detection of proteins by immunofluorescence or immunoblotting. Furthermore, optimizing insertion of epitope tags using oligonucleotide templates is almost certain to be applicable to single-base editing. Here, I describe a robust, cost effective, widely applicable method using *pha-1* co-conversion and inactivation of NHEJ repair to rapidly and precisely engineer the *C. elegans* genome using oligo-templated repair with the CRISPR/Cas9 system.

Materials and Methods

Genetics

The following strains were used in this study: N2(WT), GE24 *pha-1(e2123)* III, RB873 *lig-4(ok716)* III, which were provided by the *Caenorhabditis* Genetics Center. N2 animals and *lig-4* mutants were propagated at 20°, while *pha-1(e2123)* mutants were propagated at 15°. Animals were maintained on nematode growth medium seeded with *Escherichia coli* OP50 (Brenner 1974). For later injection experiments, *pha-1(e2123)* mutants were maintained on HB101. Growth conditions for each experiment are indicated in figure and table legends. Strains generated for this study are listed in Supporting Information, File S1, Table S1.

Microinjection

Mixtures of plasmids and oligos were microinjected into the gonad of young adult animals. Plasmids were purified using a Qiagen midiprep kit. Oligos were resuspended in TE buffer and working stocks of 2 μg/μl were made with nuclease-free dH_20. Repair template oligos are listed in Table S2. For PCR-generated P*U6*::*sgRNA* templates, PCR products were purified from 100-μl reactions and concentrated 10-fold using a DNA Clean and Concentrator kit (Zymo Research, no. D4004).

MfeI deletion assay

Wild-type (WT) animals were microinjected with 50 ng/μl of pJW1138 or pJW1236 [*klp-12* targeting CRISPR/Cas9 plasmids with original and flipped plus extended (F+E) sgRNAs, respectively], 10 ng/μl *myo-2*::*tdTomato* co-injection marker, and 40 ng/μl of pBluescript DNA. Marker positive F_1 animals were picked into 30 μl of M9 + gelatin in a 96 well. Concentrated OP50 food (30 μl; see the "PCR-based knock-in screening" protocol (File S1) in the for recipe) was then added and F_1's were incubated for 3–4 days at 25° to allow progeny to develop. Worms were lysed and genotyped as

described in the *PCR-based knock-in screening* section (see Supporting Information). To each 10 μl PCR, 5 μl of *Mfe*I-HF (NEB, R3589L) digestion mixture (1 μl 10× CutSmart buffer, 3.5 μl dH20, 0.5 μl *Mfe*I-HF) was added. The reaction was mixed, incubated at 37° for 1 hr, and then resolved on a 1.5% TAE-agarose gel.

Temperature-sensitive pha-1 co-conversion screening

For temperature-sensitive *pha-1* [*pha-1(ts)*] co-conversion experiments, animals were microinjected with 60 ng/μl of pJW1285 (*pha-1* targeting) CRISPR/Cas9 plasmid, 60 ng/μl of either pJW1285 (*nhr-23* PAM no. 1 targeting), or pJW1268 (*nhr-23* PAM no. 2 targeting) Cas9 plasmid and 50 ng/μl of the appropriate repair oligos. In experiments where a co-injection marker was included, *myo-2*::*tdTomato* was used at 10 ng/μl. PCR-derived P*U6*::*sgRNA* templates were injected at a concentration of 25 ng/μl along with 50 ng/μl of pJW1285 (*pha-1* targeting CRISPR/Cas9) and 50 ng/μl of the appropriate repair oligos. Injected adults grown at the permissive temperature (15°) were singled into wells of a 24-well plate containing NGM-lite agar and seeded with OP50, shifted to 25°, and incubated for 3–4 days. Rescued F_1's (L3s to adults) were the only animals other than the P0 animals observed in wells. These F_1 rescues were singled onto individual plates and incubated for two days to allow progeny development. The parental F_1 animals were then genotyped by restriction digestion, as described below, to identify animals with a *2×FLAG* insertion. The remaining PCR product was purified using a DNA Clean and Concentrator kit (Zymo Research) and then sequenced using knock-in specific primers (Table S3). To recover homozygotes for sequence-verified knock-ins, 12–24 F_2 progeny were singled onto individual plates, incubated at 25° for 2 days, and the parental F_2 was genotyped to confirm the *2×FLAG* insertion. These progeny were also genotyped for *pha-1(ts)* repair by PCR and CEL-1 digestion followed by sequencing of candidate repair homozygotes.

Genotyping PCRs and restriction digestion

Single F_1 animals were picked into 10 μl of single-worm lysis buffer [10 mM Tris (pH 8.3), 50 mM KCl, 2.5 mM $MgCl_2$, 0.45% IGEPAL, 0.45% Tween-20] containing 1 mg/ml proteinase K. Tubes were incubated on dry ice for 15 min, 62° for 1 hr, and then heated to 95° for 20 min to inactivate the proteinase K. Genotyping PCRs were performed using Phusion polymerase (NEB, no. M0530S) and High Fidelity buffer; 1/10 volume of lysate was used as template in the PCR. For identification of knock-in events in the F_1, 30-μl PCRs were performed. Five microliters of this PCR was removed and *Bam*HI digested by adding 10 μl of digestion mix per PCR (1 μl 10× NEBuffer 3, 0.5 μl *Bam*HI, and 8.5 μl dH20) and digesting for 1 hr at 37° before resolving on a 1.5% TAE-agarose gel. CEL-1 was purified from four heads of nonorganic celery (Safeway) with the celery juice extracted with a BJE510XL 900W juicer (Breville). Purification was performed as described (Yang *et al.* 2000) to the end of dialysis in step I, as described by Lo *et al.* (2013). For CEL-1 digestions, 10 μl of enzyme mix (2 μl CEL-1 + 2 μl 5xPhusion High Fidelity buffer + 6 μl dH20) was added to the 5-μl PCR and incubated at 42° for 1 hr prior to resolving on a 1.5% TAE-agarose gel, as described above. Oligos used for genotyping are listed in Table S3.

Vector generation

pJW1138 (*klp-12* targeting CRISPR/Cas9) and pJW1185 (*nhr-25* targeting CRISPR/Cas9) were derived from pDD162 using a Q5 Mutagenesis kit (NEB, no. E0554S) as previously described (Dickinson *et al.* 2013). sgRNA(F+E) was synthesized as a gene fragment (IDT gBlock; sequence in Table S4) with a Y61A9LA.1 targeting sequence (Friedland *et al.* 2013) and introduced into a pDD162-derived vector by Gibson cloning (NEB, no. E5510S) to generate pJW1219. pJW1236 (*klp-12* targeting CRISPR/Cas9), pJW1254 (*nhr-23* PAM no. 1 targeting CRISPR/Cas9), pJW1268 (*nhr-23* PAM no. 2 targeting CRISPR/Cas9) and pJW1285 (*pha-1* targeting CRISPR/Cas9) were derived from pJW1219 [CRISPR/Cas9 with sgRNA (F+E)] through Q5 mutagenesis. The *nhr-23*, *nhr-25*, and *pha-1* PAMs were manually chosen by searching for an NGG sequence in either strand close to the desired insertion site; these sgRNA target sites were then checked for specificity using the http://crispr.mit.edu website. All target sites scored >90 with no off-target sites in genes. The P*U6*::*sgRNA* template sequence was deleted from the pJW1219 vector using Q5 mutagenesis to generate pJW1259. All plasmids (standard vector propagation, and those generated by Gibson assembly, Q5 site-directed mutagenesis, or TOPO-blunt cloning) were transformed into PEG/DMSO DH5 alpha competent cells (protocol in File S1) made in house. pJW1219, pJW1259, pJW1285, pJW1310, and pJW1311 are available through AddGene.

Generation of U6 promoter::sgRNA templates by PCR

The *U6* promoter and chimeric sgRNA(F+E) template were amplified from pJW1219 and cloned into the pCR-Blunt II-TOPO vector (Invitrogen, no. K2800-20) to generate pJW1310 and pJW1311, respectively. The *U6* promoter was then PCR amplified from pJW1310 with oligos 1787 and 1788, while the sgRNA template was amplified from pJW1311 with oligo 1790 and a target-specific 60mer that contained 20 bp of homology to the *U6* promoter, 20 bp of new sgRNA target sequence, and 20 bp of homology to the sgRNA template (Table S3). New sgRNA template primers can be made by replacing the N_{20} in the following sequence with 20 bp of target specific sequence: 5′-cctcctattgcga gatgtcttg(N_{20})gtttaagagctatgctgg-3′. The *U6* promoter and sgRNA template PCRs were mixed (0.5 μl each per 100 μl PCR reaction) and amplified using the external primers (1787 and 1790; Table S3). The cycling parameters were: (i) 98° denaturation; (ii) 35 cycles of 98° for 10 sec, 61° for 30 sec, 72° for 20 sec; and (iii) 72° for 1-min final extension. To generate more P*U6*::*sgRNA* templates, the fused product was used in a 100-μl nested reaction with primers 1793 and 1794 (Table S3).

RNAi

Feeding RNAi was performed as described (Kamath *et al.* 2001; Ward *et al.* 2014). Four gravid *pha-1(ts)* adults were placed on 6-cm plates freshly seeded with HT115 bacteria expressing control or *cku-80* dsRNA, obtained from the Ahringer library (Kamath *et al.* 2003). Adults were ready to inject on the RNAi plates 4–6 days later. For each experiment *pha-1(ts)* mutants were also put on plates seeded with bacteria expressing *nhr-25* dsRNA. RNAi efficacy was confirmed by observing molting defects, protruding vulvae, abnormal germlines, and sterility arising from *nhr-25* inactivation (Asahina *et al.* 2000; Gissendanner and Sluder 2000; Brooks *et al.* 2003; Chen *et al.* 2004).

Immunoblotting

Lysates were generated as described in File S1 and resolved on Mini-PROTEAN TGX stain-free 4–15% gradient gels (Bio-Rad, no. 456-8086). Stain-free gels (Bio-Rad) contain a compound evenly distributed in the precast acrylamide gel that reacts with tryptophan following UV exposure and gives a strong fluorescent signal that can be used to stain for total-protein levels in acrylamide gels, monitor transfer in immunoblotting, and serve as a loading control. Following resolution, the stain-free compound was activated (Posch *et al.* 2013) and proteins were transferred to an Immobilon FL PVDF membrane (Millipore, no. IPFL00010) at 100 V for 60 min. Total protein, pre- and post-transfer, was monitored using the stain-free fluorophore as described (Posch *et al.* 2013). Stain-free imaging of total protein was used to confirm equal loading. The blots were sequentially probed with anti-FLAG (1:1000) (M2 clone, Sigma, no. F1504), and sheep antimouse–HRP conjugate (1:5000) (GE Healthcare, no. RPN4201). WesternBright Sirius HRP substrate (Advansta, no. K-12043-C20) and ECL Prime (GE Healthcare, no. RPN2232) were used to develop the blots in Figures 2 and 5, respectively. All blots were imaged using a ChemiDoc MP imaging system (Bio-Rad).

Accession codes

The accession codes are as follows: pJW1219 [Cas9-sgRNA(F+E) targeting site in Y61A9LA.1, AddGene plasmid 61250]; pJW1259 (Cas9 plasmid with sgRNA deleted, AddGene plasmid 61251); pJW1285 [Cas9-sgRNA(F+E) targeting site in *pha-1*, AddGene plasmid 61252]; pJW1310 (*U6* promoter template vector; AddGene plasmid 61253); and pJW1311 [sgRNA(F+E) template vector, AddGene plasmid 61254].

Additional methods are described in Supporting Information.

Results and Discussion

sgRNA(F+E) displays increased activity relative to the original sgRNA in deleting an MfeI restriction site in the klp-12 gene

Initial reports describing use of oligos to introduce single-base changes reported edits in 0.7–3.5% of the F_1 progeny screened (Zhao *et al.* 2014). Recent work in mammalian cells reported that a modified sgRNA(F+E), with an extended Cas9 binding structure and removal of a potential PolIII terminator by an A-U basepair flip, exhibits improved activity (Chen *et al.* 2013a). I therefore tested whether this modified sgRNA(F+E) displayed increased activity in *C. elegans*, as a potential tool to improve editing efficiency. The modified sgRNA was introduced into the pDD162 CRISPR/Cas9 plasmid (Dickinson *et al.* 2013), and to evaluate sgRNA activity, deletion of an *Mfe*I restriction site in the *klp-12* gene (Friedland *et al.* 2013) was used as a readout (Figure S1). sgRNA(F+E) produced a significant increase in deletion of the *Mfe*I site in animals positive for the co-injection marker (Table 1), and was used for all subsequent experiments.

pha-1(ts) co-conversion increases knock-in efficiency with minimal handling

Having increased sgRNA activity, I next turned to improving the screening process. Two recent reports describe that selection for a visible phenotype produced by a CRISPR/Cas9 triggered editing event [*i.e.*, *unc-22* mutation or *dpy-10(cn64)* knock-in] results in an increase in knock-out and knock-in efficiencies at other genomic loci (Arribere *et al.* 2014; Kim *et al.* 2014). These approaches can be used in any genetic background, but require outcrossing or meiotic segregation of the selective mutation. My aim was to develop a stringent system with minimal handling and no outcrossing or meiotic segregation of selection markers required. *pha-1(e2123)* is a temperature-sensitive embryonic lethal mutation; mutants are viable at 15°, but display embryonic and early larval lethality when cultivated at 25° (Schnabel *et al.* 1991; Granato *et al.* 1994). *pha-1(e2123)* has been previously used to select and propagate extrachromosomal arrays carrying a *pha-1(+)* marker (Granato *et al.* 1994). *pha-1(ts)* mutants display a low spontaneous reversion frequency of 2.5×10^{-5} per haploid genome (Schnabel *et al.* 1991); the stringency of this selection was confirmed by plating 144 gravid adults and shifting them to 25°; no viable progeny were produced, only dead eggs and arrested larvae.

I selected a CRISPR/Cas9 target site that would produce a DSB 17 bp 3′ from the *e2123* point mutation and designed an 80mer repair oligo with the PAM silently mutated to prevent recleavage of the site in an edited animal (Figure 1A). Twelve WT animals were injected with the CRISPR/Cas9 plasmid, a co-injection marker, and a commercially purchased, PAGE purified repair 80mer. Eight rescued F_1's were recovered, all heterozygotes for *pha-1(ts)* repair (data not shown). Although all eight F_1's were positive for the co-injection marker, in later experiments, I also observed *pha-1(ts)* rescue in marker-negative animals. Thus, as previously observed (Arribere *et al.* 2014; Zhao *et al.* 2014), heritable transgenesis is not a prerequisite for efficient editing. Oligo-mediated repair of *pha-1(ts)* allowed recovery of repair heterozygotes, and the complete penetrance of the *e2123* embryonic lethality meant that only F_1 heterozygotes (*i.e.*, rescued animals) would develop, making screening extremely rapid.

Table 1 sgRNA(F+E) has increased activity relative to the original sgRNA in deleting an *Mfe*I restriction site in the *klp-12* gene

Genotype	Guide RNA	% deletion[a] (±95% CI)	*N*
WT	Original sgRNA	54 (±2.73)	157[b]
WT	sgRNA(F+E)	83 (±0.31)*	85[c]

N = number of co-injection marker positive F_1 progeny screened.
[a] (Number of animals with loss of *Mfe*I restriction site/total number of co-injection marker positive animals screened) × 100; CI, confidence interval; 95% confidence interval, $Z\sigma/\sqrt{n} = 1.96\sigma/\sqrt{n}$. *Two-tailed *t*-test comparing original sgRNA to sgRNA (F+E) $P = 0.043$.
[b] From four independent injections.
[c] From two independent injections.

A homozygote for *pha-1(ts)* repair had no significant difference in brood size compared to a WT control (Table S5; two-tailed *t*-test, $P = 0.75$).

I next tested whether *pha-1(ts)* repair could be used to enrich for knock-in of a *2×FLAG* oligo into the 3′ end of the *nhr-23* gene (Figure 1B), a nuclear hormone receptor involved in molting and embryonic development (Kostrouchova *et al.* 1998, 2001). I identified two potential PAMs near the desired insertion site that could be silently mutated (Figure 1B). I designed a 200mer oligo to insert a *2×FLAG* epitope just before the stop codon. As half of sgRNAs have been reported to fail in *C. elegans* (Kim *et al.* 2014), I mutated two PAMs in the oligo to allow knock-in attempts with different sgRNAs. An 18-bp linker sequence encoding the flexible linker peptide glycine-serine-4xglycine (GSGGGG; Figure 1B) was included to spatially separate the 2×FLAG tag from the NHR-23 C terminus, potentially facilitating accessibility of the tag for immunoprecipitation. Additionally, the tag encoded a *Bam*HI restriction site, which was used for diagnostic restriction digestion in PCR-based screening (Figure 1B). I injected a CRISPR/Cas9 plasmid targeting *pha-1*, an *nhr-23* CRISPR/Cas9 construct targeting the PAM nearest the stop codon (PAM no. 1; Figure 1B), the 80mer *pha-1(ts)* repair oligo (Figure 1A), and the 200mer *nhr-23:2×FLAG* oligo (Figure 1B); this oligo was not PAGE purified to test whether PAGE purification was a necessary cost. From 16 viable injected P0 animals, nine *pha-1(ts)* rescued F_1 progeny were obtained (Figure 1D). These animals were plated, allowed to self-fertilize, and then single-worm genotyping was performed (Figure 1C). Two of these nine animals were heterozygous for a potential *2×FLAG* insertion by diagnostic digest, of which one was a correct insertion; the other candidate had a frameshift in the 2×FLAG epitope. F_2 progeny of the animal carrying the precise 2×FLAG knock-in were singled and a homozygote for both the insertion and the repaired *pha-1(ts)* allele was obtained; both knock-ins were confirmed by sequencing. Brood-size analysis of a representative knock-in confirmed viability with no phenotype, indicative of *nhr-23* loss of function (*i.e.*, molting defects or high embryonic lethality) (Table S5).

To distinguish between *pha-1(ts)* repair homozygotes and heterozygotes without sequencing, I used CEL-1 digestion of PCR products (Figure S2). CEL-1 is a celery endonuclease that recognizes and cleaves mismatches in double-stranded DNA (dsDNA) formed from single nucleotide polymorphisms or small insertions or deletions (Yang *et al.* 2000; Wood *et al.* 2011). In this assay, PCRs from repair heterozygotes will lead to a digestion product (Figure S2). Normally, the absence of digestion could indicate that the animals were homozygous for either the *ts* allele or the repaired allele. However, growth at the restrictive temperature eliminates all *ts* homozygotes; therefore, all undigested PCR products are repair homozygotes. The genotypes predicted by CEL-1 digestion were confirmed by sequencing. CEL-1 or other mismatch cutting nucleases such as mung bean nuclease or T7E1 represent an efficient method to monitor single-basepair changes and help reduce the number of animals that need to be sequenced to identify homozygous knocked-in point mutations.

Short oligos are effective templates for gene conversion

The stringency of *pha-1* co-conversion offered a powerful tool to optimize oligo editing parameters. As much experimental effort was spent isolating homozygotes to confirm correct epitope insertion, I designed primers that allowed sequencing of the 2×FLAG tag in heterozygotes. These primers bound the insertion junction, with the two 3′-most bases binding to the inserted sequence (Figure S3). In some cases, poor sequencing quality made it difficult to confirm the sequence in the center of the epitope; in these cases, a separate PCR was performed using the epitope-specific primer and an external primer and sequencing was performed on this purified PCR product using the external primer. Screening in heterozygotes greatly reduced hands-on effort required to identify correct insertions.

I next tested whether oligo length (200mer, 80mer, and 60mer) affected repair efficiency. The 80mer was PAGE purified, but the 200mer and 60mers were not. These oligos were all sense in relation to the *pha-1* coding strand. The 80mer and 200mer produced similar numbers of *pha-1* rescued F_1's (9 and 12, respectively) and with the 80mer producing one *nhr-23:2×FLAG* insertion and the 200mer producing four insertions (Figure 1D). Interestingly, I observed a high percentage of males in the *pha-1(ts)* repaired F_1, generated using the 200mer (Table S6). Despite the 60mer only producing three *pha-1* rescues, two of those F_1 also had knock-ins at the *nhr-23* locus. One knock-in was incomplete and produced a frameshift; the other had an extra insertion after the 2×FLAG tag, but frame was maintained. I confirmed the expression of the 2×FLAG tag by immunoblotting in five knock-in lines carrying a precise insertion of the *2×FLAG* tag, as well as a line that contained an imprecise insertion. All five precise knock-ins expressed the FLAG tag, whereas no band was seen for the strain carrying the frameshifted FLAG tag (Figure 2). *pha-1(ts)* co-conversion allowed isolation of sequence-verified homozygotes for a knock-in event within 8–9 days.

Additional repair template considerations

I then examined whether oligo polarity had an impact on editing, using a PAGE purified, antisense version of the 80mer

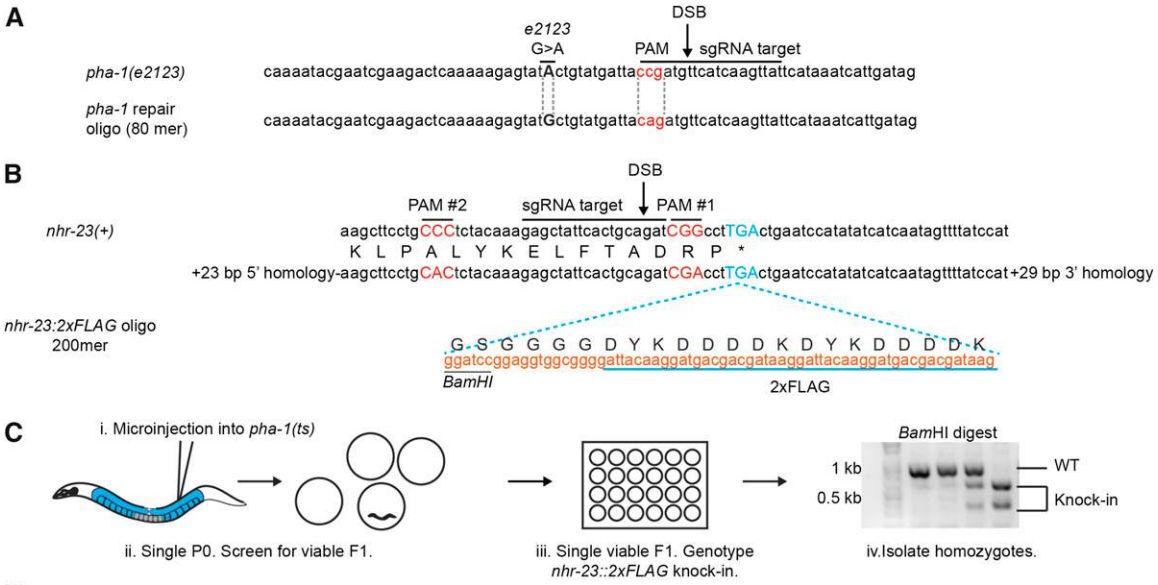

D

P0 strain	*pha-1* oligo	*nhr-23::2xFLAG* oligo	Viable injected P0	Rescued F1	P0 with rescued F1	PCR hits	Precise Knockins	% Knockins/ rescued F1	% Knockins/ P0
pha-1(ts)	80mer sense	sense	16	9	3	2	1	11	8
pha-1(ts)	80mer antisense	sense	47	3	3	1	1	33	2
pha-1(ts)	60mer sense	sense	11	3	3	2	1	33	9
pha-1(ts)	200mer sense	sense	28	12	10	5	4	33	14
pha-1(ts)	200mer sense	antisense	57	5	4	1	0	0	0

Figure 1 Selection for *pha-1(ts)* oligo-mediated repair enriches for *nhr-23*::*2×FLAG* knock-in. (A) Sequence of the *pha-1(e2123)* genomic locus targeted, with the PAM (red text), *e2123* G-to-A mutation (boldface text and underline), sgRNA target sequence, and position of the DSB indicated. The 80mer repair oligo also contains a silent C-to-A mutation to inactivate the PAM. (B) Sequence of the *nhr-23* genomic locus targeted. The stop codon (blue text), PAM (no. 1, red text) and sgRNA target, the DSB position, and an alternate PAM (no. 2, red text) are indicated. The 200mer repair oligo was designed to insert a 2×FLAG epitope with a flexible GSGGGG linker sequence, which also contains a *Bam*HI site. The oligo contains silent C-to-A and G-to-A mutations to inactivate the two indicated PAMs. (C) (i) *pha-1(ts)* mutants propagated at the permissive temperature were injected with 60 ng/μl each of CRISPR/Cas9 plasmids targeting the PAM in *pha-1(ts)* and PAM no. 1 in *nhr-23*, 50 ng/μl of an oligo designed to correct the *pha-1(ts)* allele, and 50 ng/μl of the 200mer *nhr-23*::*2×FLAG* repair oligo. (ii) P0 animals were singled onto individual plates and shifted to the restrictive temperature (25°). (iii) Three to four days later, the plates were screened for the presence of viable progeny (L3s to adults); the *e2123* embryonic lethality phenotype is completely penetrant at 25°, and only rescued animals develop. Rescued F_1 progeny were singled onto individual plates, allowed to lay eggs (2–3 days), and the parental F_1 was genotyped by PCR followed by *Bam*HI digestion. Correct insertion of the epitope is confirmed by sequencing-purified PCR products with knock-in-specific primers. (iv) Homozygotes were recovered by plating 12–24 progeny from candidate *nhr-23:2×FLAG* knock-in F_1's, allowing them to lay eggs (2–3 days), and genotyping the parental F_2 animal by PCR and *Bam*HI digestion. Marker size in kilobases is provided. (D) Summary of *pha-1(ts)* co-conversion experiments. Viable P0 are the number of injected animals that produced eggs; a variable number of animals are sterile in each experiment. The length and polarity (with respect to the coding strand) of the *pha-1(ts)* repair and *nhr-23*::*2×FLAG* oligos are provided. P0 were propagated on OP50 *E. coli* for these injections.

pha-1(ts) repair oligo. The sense oligo was homologous to the coding DNA strand, whereas the antisense oligo was homologous to the template DNA strand. The antisense oligo produced the fewest knock-ins per viable P0 animal of all conditions tested, but still had a high rate of *nhr-23*::*2×FLAG* knock-in per rescued F_1 (Figure 1D). Thus, it appeared to be a poor repair template for *pha-1(ts)* repair, but once this repair event was selected could still lead to enrichment in *nhr-23*::*2×FLAG* knock-in. To further explore this variable, I tested whether *nhr-23*::*2×FLAG* could be knocked in using an antisense 200mer. Using a sense *pha-1* 200mer, five rescued F_1's were obtained from 57 viable P0 animals, but no *nhr-23*::*2×FLAG* knock-ins were detected (Figure 1D). Including the antisense 200mer with the sense 200mer did result in a decrease in knock-in efficiency (1/5 *vs.* 1/9), but more animals need to be screened to determine if this effect is significant (Figure S4). Interestingly, when annealed *nhr-23*::*2×FLAG* sense and antisense oligos were injected, no knock-ins were recovered, indicating that dsDNA is not a better template than single-stranded DNA (ssDNA) and may be less effective (Figure S4). These data suggest that the strand to which oligo homology is derived could be an important parameter for editing efficiency and that ssDNA may be more effective than dsDNA for epitope knock-in. However, these inferences must be tested with many additional combinations of sgRNAs, loci, and repair templates to assess their generality.

Growth on HB101 suppresses pha-1(ts) low brood size and sterility

A number of injected P0s in these experiments were sterile. This sterility could have been a consequence of injection trauma or general sickness of *pha-1(ts)* mutants. To discriminate

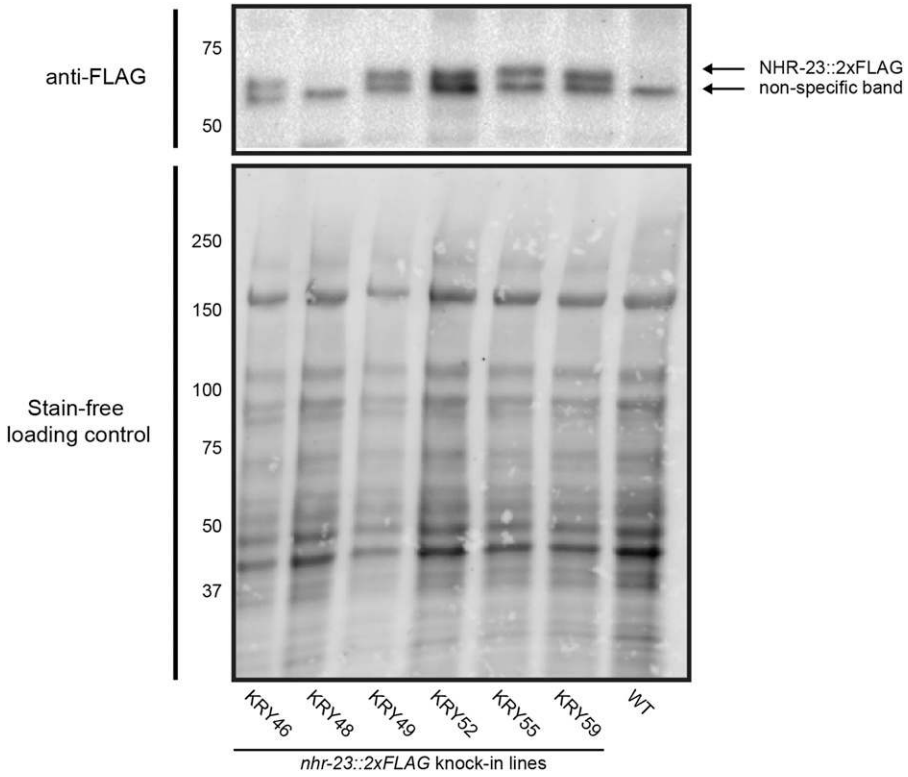

Figure 2 Detection of NHR-23::2×FLAG in precise knock-ins. Four micrograms of protein from synchronized gravid adults of the indicated strains was analyzed by immunoblotting with anti-FLAG. KRY48 contains a frameshift in the 2×FLAG tag and thus does not express the epitope. Stain-free (Bio-Rad) analysis of total protein on the blot is provided as a loading control. Marker size (in kilodaltons) is provided.

between these possibilities, I shifted adult *pha-1(ts)* mutants to 25° to mimic the selection protocol. Interestingly, these animals displayed sterility (1/24 P0) and low brood sizes (<10 eggs) in 6 of 24 P0s. Growth on HB101 has been shown to suppress the slow growth rate of *eat-2 (ad465)* and *eat-5 (ad1402)* mutants, which have defective pharyngeal pumping (Shtonda and Avery 2006). Moreover, *unc-119(ed3)* strains are frequently grown on HB101 in genome editing protocols to ameliorate sickness of that strain (Frøkjær-Jensen *et al.* 2010; Dickinson *et al.* 2013). I therefore tested the effect of HB101 growth on *pha-1(ts)* mutants by propagating animals for several generations on HB101 at 15°, then picking adult animals and shifting them to 25°. Growth on HB101 suppressed the low brood size and sterility observed during growth on OP50. *pha-1(ts)* mutants grown on HB101 and then shifted to OP50 at L4 had brood sizes of 127 ± 34 (Table S5) with 0% viable progeny. Subsequently, the *pha-1(ts)* strain was maintained on HB101 at 15° prior to micro-injection.

A PCR fusion method to rapidly generate new sgRNA templates

Having demonstrated that oligo-mediated repair of the *pha-1(e2123)* mutation can be used to efficiently enrich for knock-ins at other loci, I next turned to optimizing sgRNA delivery. Generation of new sgRNA templates for plasmid-based CRISPR/Cas9 systems typically involves site-directed mutagenesis (Dickinson *et al.* 2013) or cloning using oligonucleotides (Waaijers *et al.* 2013) or PCR products (Friedland *et al.* 2013; Kim *et al.* 2014). A major impediment to the success of a CRISPR/Cas9 experiment is the efficiency of the sgRNA; Kim *et al.* (2014) report that half of their tested sgRNAs fail. Given that efficient promoter::GFP reporters can be generated by fusion PCR (Hobert 2002), I tested whether the same approach could be used to express sgRNAs from the *U6* promoter. This approach would allow rapid screening of sgRNAs, as PCR templates could be injected on the same day of amplification without need for cloning or transformation. For cost efficiency, four PCR primers were used, of which only one is changed to generate a new P*U6*::*sgRNA* template (Figure 3A). As a proof of principle, I generated P*U6*::*sgRNA* template fusions targeting *pha-1* and *nhr-23* PAM no. 1, and deleted the sgRNA template sequence from the pJW1219 Cas9/CRISPR plasmid. Injecting this Cas9 plasmid (pJW1259), the PCR-generated *pha-1* and *nhr-23* P*U6*::*sgRNA* templates, the *pha-1(ts)* sense 80mer repair template, and the *nhr-23*::*2×FLAG* sense 200mer, efficient knock-in at both loci with comparable frequency to the corresponding plasmid-based P*U6*::sgRNA templates was observed (Figure 3B). Fusion PCR thus allows rapid, cost-effective generation of sgRNA templates driven by the *U6* promoter.

DSBs up to 54 bp from the insertion site can generate nhr-23::2×FLAG knock-ins

During my initial design of the *nhr-23*::*2×FLAG* repair oligo, I mutated two potential PAMs, as it has been reported that half of all sgRNAs fail; this single oligo would allow testing of two separate sgRNAs (Kim *et al.* 2014). While analyzing the sequence of the 22 candidate *nhr-23*::*2×FLAG* knock-ins generated using sgRNAs targeting PAM no.1 and identified by *Bam*HI digest (Figure 1D, Figure 3B, Table 2), I observed co-conversion of the PAM no. 2 silent mutation in six lines.

A

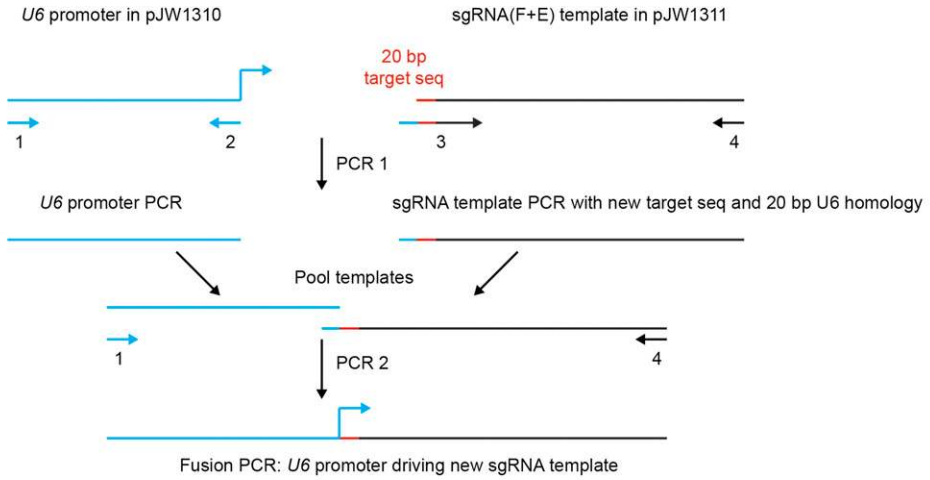

B

P0 strain	pha-1 oligo	Viable injected P0	Rescued F1	P0 with rescued F1	PCR hits	Precise Knockins	% Knockins/ rescued F1	% Knockins/ P0
pha-1(ts)	200mer sense	27	6	3	4	1	16.67	3.70

Figure 3 PCR generated sgRNA templates can be used for *pha-1(ts)* co-conversion. (A) Method for generating P*U6*::*sgRNA* templates by PCR. The *U6* promoter and sgRNA template were separately subcloned to generate pJW1310 and 1311, respectively. The *U6* promoter is amplified with oligos 1 and 2, and the sgRNA template is amplified with oligos 3 and 4. Oligo 3 contains 20 bp of homology to the sgRNA template, the new 20 bp sgRNA targeting sequence, and 20 bp of homology to the *U6* promoter. The resulting P*U6* and sgRNA template PCR products are then mixed and used as template in a second PCR reaction using oligos 1 + 4. (B) Animals were injected with 60 ng/μl of the Cas9 plasmid, 25 ng/μl each of PCR generated P*U6*::*sgRNA* templates targeting *pha-1* and *nhr-23* (same targeting sequence as in Figure 2), and 50 ng/μl each of the 200mer sense *pha-1(ts)* repair oligo and *nhr-23*::*2×FLAG* oligo. Viable P0 are the number of injected animals that produced eggs; a variable number of animals are sterile in each experiment. P0 were propagated on HB101 *E. coli* for these injections. Oligo polarity (sense) is with respect to the coding strand.

These co-conversion events suggested that *pha-1(ts)* selection could be used to explore gene conversion track lengths and effectiveness of DSB position relative to the insertion site.

The silent point mutations in PAMs no. 1 and no. 2 were 29 bp apart, which agrees with my observation that a 60mer with 29 bp of homology can be used to efficiently knock-in point mutations (Figures 1D and Figure 4A). For these next experiments, I sequenced all *pha-1(ts)* rescued F_1's. I first tested whether an sgRNA targeting PAM no. 2 could be used to knock in the *2×FLAG* tag into the *nhr-23* 3′ end; 3 of 12 *pha-1(ts)*-rescued F_1 animals had the PAM no. 2 mutation knocked in, with one animal also containing the PAM no. 1 mutation and correct insertion of the 2×FLAG tag (Figure 4B, Table S7). I next examined whether a DSB 54 bp away from the desired insertion site could be used to knock in the *2×FLAG* epitope (Figure 4A). I designed a modified version of the 200mer used for the above experiment that also carried three silent mutations to disrupt the sgRNA binding to the PAM no. 3 target site, as well as the mutations in PAMs no. 1 and no. 2 (Figure 4A). A fourth potential PAM (no. 4) was left intact in the repair template, as inactivation would leave only 10 bp of 5′ homology; this sgRNA was inactive (Figure 4, A and B). Using an sgRNA targeting PAM no. 3 to generate a DSB, two of eight *pha-1(ts)*-rescued F_1's carried the silent mutation in PAM no. 3; the others all had wild-type sequence, suggesting that this may be an inefficient sgRNA (Figure 4B, Table S7). Of the two animals with mutations in PAM no. 3, both had the PAM no. 2 inactivating mutation, and one had the PAM no. 1 mutation and insertion of the 2×FLAG tag (Table S7). Though there was a 1-bp deletion within the tag, this experiment demonstrates that a DSB 54 bp from an insertion site can be used for introduction of epitopes, and that the presence of mutations in a stretch of homology does not prevent gene conversion; five point mutations in a 55-bp stretch were introduced into the genome along with the 65 bp of 2×FLAG tag (with the 1-bp deletion). Animals were not tracked to identify originating P0s; however, for the PAM no. 1 knock-in experiment, the six animals with PAM no. 2 mutation co-conversion were isolated from six different injections, and thus represent independent events (Figure 4B). Knock-in efficiency appeared higher the closer the DSB was to the insertion site, but sgRNA efficiency could also play a role in this observation.

Homology arms of 35 bp are sufficient for oligo-templated insertion of a 2×FLAG tag

Exploring DSB position relative to the insertion site demonstrated that the stringency of *pha-1(ts)* co-conversion combined with the speed and ease in recovering editing events allowed rapid testing of editing parameters. Interestingly, the 200mer used for the PAM no. 3 knock-in experiments only had 29 bp of homology 5′ to the DSB (Figure 4, A and B), suggesting that homology arms could be relatively short. Efficient repair of the *pha-1(ts)* allele was observed using a 60mer with 29 bp of homology (Figure 1D). Furthermore, recent data using PCR-derived dsDNA repair templates demonstrated

Table 2 *cku-80* RNAi results in increased knock-in efficiency

P0 strain	*pha-1* oligo	Repair oligo	Viable injected P0	*pha-1* rescued F_1	P0 with rescued F_1	PCR hits	Knock-ins	Knock-ins/F_1 rescue (%)	Knock-ins/P0 (%)
pha-1(ts); *control(RNAi)*[a]	80mer	*nhr-23*::*2×FLAG*	10	1	1	1	1	100.0	10.0
pha-1(ts); *cku-80(RNAi)*[a]	80mer	*nhr-23*::*2×FLAG*	16	10	6	6	5	50.0	31.3
pha-1(ts); *control(RNAi)*[b]	200mer	*nhr-25*::*2×FLAG*	21	7	4	0	0	0.0	0.0
pha-1(ts); *cku-80(RNAi)*[b]	200mer	*nhr-25*::*2×FLAG*	22	36	12	5	4	11.1	18.2
pha-1(ts); *control(RNAi)*[b]	200mer	*nhr-23*::*3xFLAG*	34	7	4	1	1	14.3	3.0
		nhr-25::*3xFLAG*				1	1	14.3	3.0
pha-1(ts); *cku-80(RNAi)*[b]	200mer	*nhr-23*::*3xFLAG*	13	5	3	2	2	40.0	15.4
		nhr-25::*3xFLAG*				2	1[c]	20.0	7.7
pha-1(ts); *cku-80(RNAi)*[b]	200mer	*2×FLAG*::*smo-1*	15	29	7	14	11	38.0	73.3
		lig-4 stop				0	0	0.0	0.0

Summary of *pha-1(ts)* coselection experiments testing NHEJ inactivation. The RNAi treatment of the injected P0 animals is indicated. Viable P0 are the number of injected animals that produced eggs; a variable number of animals are sterile in each experiment. The length of the *pha-1(ts)* sense repair oligo is provided. For *nhr-23*::*2×FLAG* experiments, animals were injected with 60 ng/μl each of the *pha-1* and *nhr-23* CRISPR/Cas9 plasmids, and 50 ng/μl each of the *pha-1(ts)* repair and *nhr-23*::*2×FLAG* (sense) oligos. For the remaining experiments, animals were injected with 50 ng/μl of the *pha-1* CRISPR/Cas9 plasmid, 25 ng/μl of appropriate P*U6*::*sgRNA* template PCR product, and 50 ng/μl each of the *pha-1(ts)* repair oligo and knock-in oligo.

[a] Pre-RNAi diet = OP50 *E. coli*.

[b] Pre-RNAi diet = HB101 *E. coli*.

that 30- to 60-bp homology arms were optimal, with knock-in efficiency actually decreasing with longer homology arms (Paix *et al.* 2014). To test the ideal length of homology for oligo-mediated insertion of epitopes, I designed *nhr-23*::*2×FLAG* oligos with 35 bp, 25 bp, or 15 bp of homology and tested their ability to introduce the *2×FLAG* epitope using a DSB generated by an sgRNA targeting PAM no. 1. Knock-in efficiency using these homology arms was compared to pooled data from the *pha-1(ts)* and *nhr-23*::*2×FLAG* sense oligo experiments (Figure 1D and Figure 3B). This 200mer sense *nhr-23*::*2×FLAG* oligo (Figure 1B) contained 54 bp of homology 3′ to the insertion site and 76 bp of homology 5′ to PAM no. 1 (76/54). With the 35-bp homology arms, two animals from 9 rescued F_1's had correct insertion of the *2×FLAG* epitope (Figure 4C). This 22% knock-in per F_1 screened (2 of 9) is comparable to the 26% efficiency (7 of 27) observed using the 76/54 oligo (Figure 4C). The knock-in rate per successfully injected P0 was also comparable for the 35-bp and the 76/54-bp homology arms [4.76% (2/42) *vs.* 6.86% (7/102)]. The 15- and 25-bp homology arm produced fewer *pha-1(ts)* rescues per successfully injected P0, and only the 25-bp homology arms could produce a *2×FLAG* insertion, though this knock-in carried a point mutation (Figure 4C). These data suggest that, similar to dsDNA templates, homology arms of 35–80 bp are ideal for oligo-templated editing.

Inactivation of NHEJ repair increases knock-in efficiency

In *Drosophila*, increased homologous recombination efficiency can come from inactivation of NHEJ (Beumer *et al.* 2008; Bottcher *et al.* 2014). I therefore used the *pha-1(ts)* system to test whether NHEJ inactivation impacted knock-in by homologous recombination. NHEJ mutants may have additional background mutations due to compromised repair of endogenous DSBs and would require additional outcrossing. I therefore tested the effect on knock-in frequency of temporary inactivation of the *C. elegans* homolog of Ku80 (*cku-80*), part of a heterodimer that binds the end of DSBs in NHEJ, and which had reported RNAi phenotypes (Dmitrieva *et al.* 2005; McColl *et al.* 2005). *pha-1* and *nhr-23* CRISPR/Cas9 plasmids, the *pha-1* sense 80mer repair oligo, and the *nhr-23* sense 200mer repair oligo were injected into *pha-1(ts)* mutants treated with control or *cku-80* RNAi. Control RNAi produced one *pha-1(ts)* rescued F_1, which also carried a sequence-confirmed *nhr-23* knock-in event (Table 2). However, inactivation of *cku-80* by RNAi produced an increase in both *pha-1(ts)* rescue (10 F_1's) and *nhr-23*:*2×FLAG* co-knock-ins recovered (n = 5) (Table 2). These experiments suggested that NHEJ inactivation boosts oligo-mediated knock-in efficiency.

To confirm that *pha-1(ts)* co-conversion, PCR-generated sgRNAs templates, and NHEJ inactivation were effective on other loci, I attempted to introduce a 2×FLAG epitope in *nhr-25*, a broadly expressed nuclear hormone receptor that regulates several developmental and physiological programs (Asahina *et al.* 2000; Gissendanner and Sluder 2000; Chen *et al.* 2004; Asahina *et al.* 2006; Mullaney *et al.* 2010; Ward *et al.* 2013, 2014). I selected the 3′ end of *nhr-25* as there are two isoforms that share a common 3′ end, but differ in promoter use; thus, targeting the 3′ end of *nhr-25* with the 2×FLAG should in principle allow for labeling of all known *nhr-25* isoforms. I designed a 175mer repair template with six silent point mutations in the 20-bp sequence preceding the PAM, as the PAM could not be silently mutated (Figure S5, A and B). As with the *nhr-23*::*2×FLAG* construct, an 18-bp spacer encoding with a *Bam*HI site was also included (Figure S5, A and B). This oligo contained 41 bp of homology 5′ to the mutated sgRNA target sequence and 43 bp of 3′ homologous sequence. *pha-1(ts)* mutant animals grown on either control or *cku-80* RNAi were injected with a *pha-1(ts)* CRISPR/Cas9 plasmid, an *nhr-25* P*U6*::*sgRNA* template PCR product, and *pha-1(ts)* and *nhr-25*::*2×FLAG* repair oligos. Seven *pha-1* rescues were recovered from the control RNAi-treated animals and 36 from the *cku-80* RNAi-treated animals (Table 2). No knock-in candidates were recovered from the control RNAi injection, but five were recovered

A

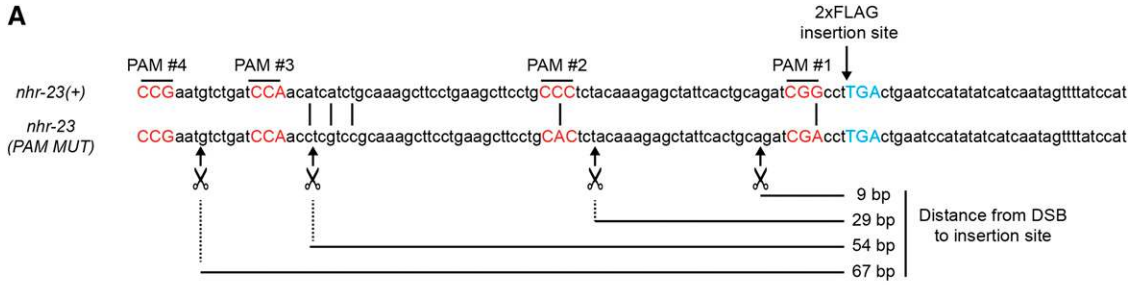

B

sgRNA	DSB Distance from insert site	Viable injected P0	F1 rescues	FLAG insertions	PAM#1	PAM#2	PAM#3
PAM #1[a]	9 bp	212	49	22[b]	22	6	n/a
PAM #2	29 bp	16	12	1	1	3	n/a
PAM #3	54 bp	13	8	1[c]	1	2	2
PAM #4	67 bp	20	7	0	0	0	0

[a]Pooled from all 200mer *nhr-23-2xFLAG* injections (Figures 1 and 3, Table 2)
[b]Includes 14 precise insertions and 8 partial insertions
[c]1 bp deletion in inserted FLAG tag
n/a-PAM mutation not in repair template

C

Homology arms (5′/3′)	Viable injected P0	*pha-1* rescued F1	P0 with rescued F1	PCR hits	Knockins	% Knockins/ *pha-1* rescue	% Knockins/ P0
76/54[a]	102	27	19	10	7	25.9	6.9
35/35	42	9	6	2	2	22.2	4.8
25/25	34	1	1	1[b]	0	0.0	0.0
15/15	21	2	1	0	0	0.0	0.0

[a]Pooled from all non-RNAi 200mer *nhr-23-2xFLAG* injections using sense oligos (Figures 1 and 3)
[b]1 bp deletion in inserted FLAG tag

Figure 4 DSBs up to 54 bp from an insertion site, and 35-bp homology arms can be used for oligo-templated repair in *nhr-23*. (A) Schematic of the *nhr-23* 3′ end, indicating the stop codon (blue text), four PAMs tested (red text), and position of the DSBs (scissor). Mutations used to inactivate PAMs in repair templates are provided in the *nhr-23(PAM MUT)* sequence and indicated by the vertical lines between the *(+)* and *(PAM MUT)* sequence. (B) Testing effect of DSB position on *nhr-23*::*2×FLAG* epitope knock-in efficiency. The PAMs for the sgRNAs used to generate the DSB and mutations used to inactivate the PAMs in the repair templates are provided in A. Animals were co-injected with 50 ng/μl of *pha-1* targeting CRISPR/Cas9 plasmid, 50 ng/μl each of the *pha-1(ts)* repair oligo and a 200mer sense *nhr-23*::*2×FLAG* repair oligo, and either 50 ng/μl of *nhr-23* targeting CRISPR/Cas9 plasmid (PAMs no. 1 or no. 2), or 25 ng/μl of P*U6*::*sgRNA* template PCR product (PAMs no. 3 and no. 4). For the PAM no. 1 and no. 2 sgRNA experiments, the repair template carried mutations in both PAMs. For the PAM no. 3 and no. 4 experiments, the repair template carried mutations in PAMs no. 1, no. 2, and no. 3. PAM no. 3 had a single PCR hit with a 2×FLAG insertion carrying a 1-bp deletion. For the PAM no. 1 row, all experiments using *nhr-23*::*2×FLAG* 200mers were pooled (Figure 1, Figure 3, Table 2); only animals that displayed a knock-in signature in the diagnostic *Bam*HI digest from these experiments were sequenced. For the PAM no. 2, no. 3, and no. 4 experiments, all *pha-1(ts)* F_1 rescued animals were sequenced. (C) Testing homology arm length on *nhr-23*::*2×FLAG* knock-in efficiency. Homology lengths in basepairs for 5′ and 3′ arms are provided. 5′ arm homology numbering starts from the middle G in PAM no. 1; 3′ homology numbering starts from the first basepair of the stop codon. Animals were co-injected with 50 ng/μl each of *pha-1* targeting and *nhr-23* PAM no. 1 targeting CRISPR/Cas9 plasmids, 50 ng/μl each of the *pha-1(ts)* repair oligo and *nhr-23*::*2×FLAG* repair oligo. For the 76/54-bp homology arm row in the table, data were pooled from all non-RNAi experiments using *pha-1* sense repair oligos and *nhr-23*::*2×FLAG* sense 200mers (Figure 1 and Figure 3). With the exception of the pooled data, all injected P0 animals were grown on HB101 *E. coli* in B and C. Oligo polarity (sense) is with respect to the coding strand.

from the *cku-80* RNAi-treated animals, of which four were correct insertions of the 2×FLAG tag (Table 2). Strikingly, one of these animals was an F_1 homozygous knock-in. These strains were viable and did not display defects associated with *nhr-25* inactivation (protruding vulvae, molting defects, embryonic lethality; see Table S5 for a representative brood size). I confirmed expression of the 2×FLAG tag in an outcrossed, representative line (Figure 5B).

Multiplexed editing using pha-1(ts) co-conversion and cku-80 RNAi

Given the efficient editing observed in *cku-80* RNAi-treated animals and the 35–80 bp of homology sufficient for oligo-templated repair, I next tested whether I could introduce larger epitopes using *pha-1(ts)* co-conversion. As Kim *et al.* (2014) had reported generating mutations in both *avr-14* and *avr-15* in one *unc-22* co-CRISPR experiment, I attempted to knock in 84-bp 3xFLAG tags containing the GSGGGG spacer into both *nhr-23* and *nhr-25* in one injection experiment (Figure S5A). From 13 successfully injected P0 animals treated with *cku-80* RNAi, two precise *nhr-23*::*3xFLAG* lines were obtained (Table 2). A viable *nhr-25*::*3xFLAG* line that expressed the 3xFLAG tag, but had a 51-bp duplication in the 3′ UTR was also obtained; as the tag was expressed and the strain was viable, this line was scored as a correct knock-in (Table 2, Table S5). A single knock-in animal was

obtained from 34 successfully injected P0 animals grown on control RNAi (Table 2). This F_1 animal was homozygous for an *nhr-25*::*3xFLAG* insertion and heterozygous for an *nhr-23*::*3xFLAG* insertion (Table 2). Viability was confirmed for representative *nhr-23*::*3xFLAG* and *nhr-25*::*3xFLAG* lines and for the *nhr-23*::*3xFLAG*; *nhr-25*::*3xFLAG* double knock-in line (Table S5). No defects consistent with *nhr-23* or *nhr-25* inactivation were observed, though the double knock-in did have a lower brood size (Table S5). I confirmed FLAG epitope expression in outcrossed *nhr-23*::*3xFLAG* lines and *nhr-25*::*3xFLAG* lines (Figure 5, A and B). The 3xFLAG epitope lines displayed a marked increase in band intensity in immunoblots compared to 2×FLAG lines, for both NHR-23 and NHR-25 (Figure 5, A and B). Notably, the *nhr-23*::*2×FLAG* epitope was not detectable in this experiment (Figure 5A), as a more potent ECL substrate was required for detection by immunoblotting (Figure 2); this more potent ECL substrate may explain the nonspecific band observed in Figure 2, but not in Figure 5A. I also observed extra bands in the 3xFLAG lines for NHR-23 and NHR-25 compared to the corresponding 2×FLAG lines, which would be consistent with NHR-23 and NHR-25 isoforms, though they could also represent degradation products (Figure 5, A and B). Comparing all NHEJ inactivation experiments, growing P0 animals on *cku-80* RNAi produced a significant increase in the number of knock-ins recovered per injection experiment (two tailed *t*-test $P = 0.01$) and percentage of knock-ins per viable P0 (two-tailed *t*-test $P = 0.016$). No significant difference was observed in the number of P0 animals with rescued F_1 progeny (two tailed *t*-test $P = 0.16$) or in the percentage of knock-ins per rescued F_1 (two tailed *t*-test $P = 0.85$). Recent manuscripts have described a "jackpot" phenomenon (Arribere *et al.* 2014; Paix *et al.* 2014), where the majority of edits come from a small number of P0 animals. There may be a trend of "richer jackpots" in *cku-80* RNAi-treated animals with 2.6 rescued F_1's/P0 producing F_1 rescues (±0.44; 95% confidence interval) *vs.* 1.6 (±0.50; 95% confidence interval) in control RNAi-treated animals. This difference was not significant in a two-tailed *t*-test ($P = 0.19$) potentially due to the large variation in number of F_1 rescues and knock-ins produced across assays, and this observation will require further exploration.

PAGE purification of oligos is not necessary, but increases editing efficiency

The *nhr-25*::*3xFLAG* oligo appeared to be a poor repair template, as it yielded lower knock-in efficiency in comparison to the *nhr-25*::*2×FLAG* template, and complex insertions were observed in two *nhr-25*::*3xFLAG* candidate knock-in lines. Although experiments demonstrated that PAGE purification was not necessary, the *nhr-25*::*3xFLAG* template was ideal to test whether PAGE purification nonetheless increased knock-in efficiency or fidelity. Resolving unpurified and purified oligos on a denaturing TBE-Urea gel revealed that the unpurified oligo preparation contained large amounts of incorrectly sized product (Figure S6A). *pha-1(ts)* animals grown on control or *cku-80* RNAi were injected with the *pha-1* targeting CRISPR/Cas9 vector, an *nhr-25* sgRNA template PCR product, a *pha-1* repair oligo, and either purified or unpurified *nhr-25*::*3xFLAG* 175mers. Interestingly, this experiment demonstrated that PAGE purification resulted in higher rates of knock-ins per F_1 and per viable P0 (Figure S6B). Comparing all experiments using the *nhr-25*::*3xFLAG* oligos (Table 2, Figure S6C), both knock-in candidates obtained using the purified oligo were precise insertions, whereas two of the four candidates generated with the unpurified oligo contained additional sequence inserted (Figure S6C). These experiments suggested that one can either opt for an increased knock-in rate with PAGE purified oligos or avoid this cost and inject/screen more animals.

Efficient editing at other genomic loci and rapid testing of sgRNA activity using pha-1(ts) selection and NHEJ inactivation

Finally, I wished to test these editing parameters on other genes to test their general applicability and robustness. Based on my previous work on NHR-25 sumoylation (Ward *et al.* 2013), I chose a previously described weakly efficient sgRNA (Kim *et al.* 2014) that cleaved 19 bp 3′ to the start codon of the single *C. elegans* SUMO gene, *smo-1* (Broday *et al.* 2004). I designed a 175mer repair oligo to create a SMO-1 N-terminal 2×FLAG fusion (Figure S5, C and D). I also designed two overlapping sgRNAs to target the NHEJ gene, *lig-4*, and a 60mer oligo as the homologous recombination template to insert a stop codon (oligos were unpurified). From nine successfully injected P0 animals grown on *cku-80* RNAi and injected with PCR-derived sgRNA templates, 27 *pha-1(ts)* rescued F_1 animals were obtained. Fourteen of these F_1's carried knock-ins in *smo-1*, of which 11 were precise (Table 2). I confirmed the expression of the 2×FLAG epitope in a representative line (KRY82) by immunoblotting; signal was observed over a large range of molecular weights, as expected from SUMO conjugation to hundreds of substrates in *C. elegans* (Kaminsky *et al.* 2009) (Figure 5C). Although viable, *2×FLAG*::*smo-1* homozygotes displayed partially penetrant phenotypes consistent with *smo-1* reduction of function, such as small body size and protruding vulvae. Thus, epitope placement may need to be optimized in *smo-1*, though the creation of a viable hypomorph will be a useful reagent for the community. The *lig-4* sgRNAs failed, as no knock-ins or mutations were obtained in *lig-4*, demonstrating that this approach also allows rapid testing of sgRNA efficacy, similar to Kim *et al.* (2014) (Table 2). Together, these results demonstrate that a co-conversion approach using a temperature-sensitive mutant allele, PCR-generated sgRNA templates, and NHEJ inactivation by RNAi provide a flexible, robust platform to recover genome editing events.

pha-1(ts) coselection increases screening efficiency

Based on recent co-CRIPSR/co-conversion reports (Arribere *et al.* 2014; Kim *et al.* 2014), and the frequency at which relatively rare *pha-1(ts)* repair events were associated with edits at other loci, it was highly probable that *pha-1(ts)*

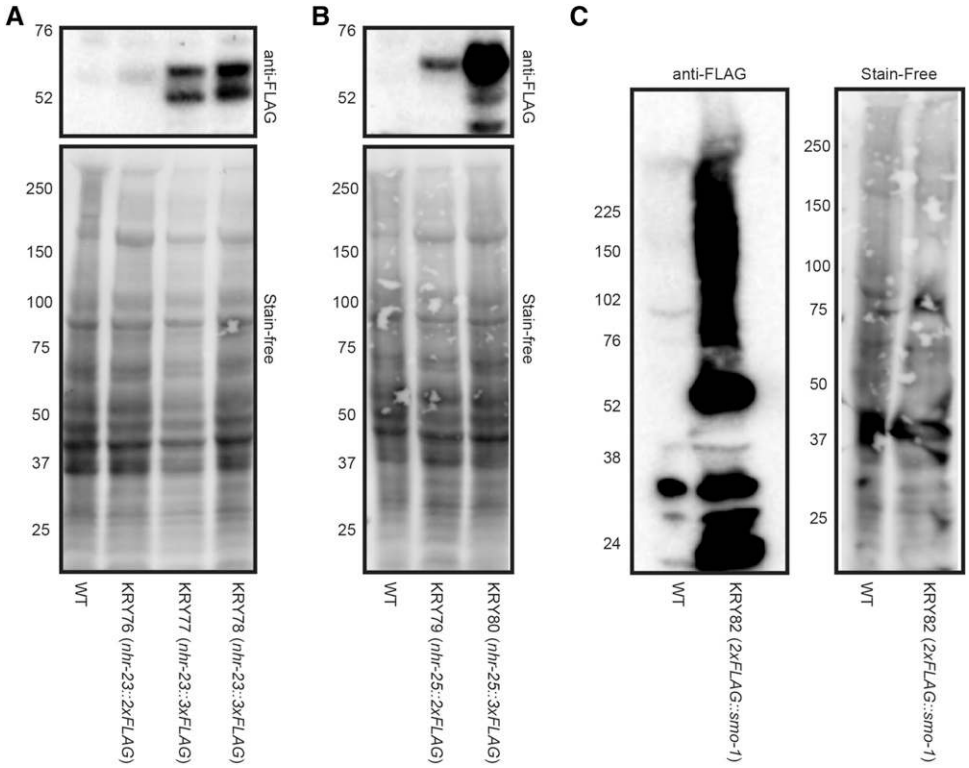

Figure 5 Detection of FLAG epitope expression in *nhr-23*-, *nhr-25*-, and *smo-1*-tagged lines. Anti-FLAG immunoblot analyses of lysates are from mixed stage animals of the indicated genotypes. The 2x and 3xFLAG tagged *nhr-23* (A) and *nhr-25* (B) lines and a *2×FLAG::smo-1* tagged line (C) were assayed. Stain-free (Bio-Rad) analysis of total protein on each blot is provided as a loading control. Marker size (in kilodaltons) is provided. The same exposure time was used to image all anti-FLAG blots. For the NHR-23 blot (A), the background band observed in Figure 2 was not detected, likely because a more potent ECL substrate was used for that experiment.

coselection increases screening efficiency. Prior to developing *pha-1(ts)* co-conversion, I had attempted to introduce 2×FLAG tags onto the 3′ end of *nhr-23* and *nhr-25* and recover knock-ins through direct screening of F_1 progeny, similar to the approach described by Paix *et al.* (2014) (see Supporting Information for detailed methods). No knock-ins were recovered from 380 screened WT F_1's (Table S8). I also tested the effect of NHEJ inactivation by injecting into *lig-4(ok716)* mutants; DNA ligase 4 (*lig-4*) encodes the enzyme that seals DSBs in canonical NHEJ, and *ok716* is an out-of-frame deletion that removes the catalytic ligase domain and is predicted to result in a premature stop codon (Clejan *et al.* 2006). A single knock-in was recovered from 768 screened *lig-4* mutant F_1's (Table S8); after outcrossing the *lig-4* mutation, this *nhr-25*::*2×FLAG* line had a brood size equivalent to a knock-in produced by *pha-1(ts)* coselection (Table S5). In comparable *pha-1(ts)* coselection experiments, no knock-ins were recovered from 7 F_1 laid by control RNAi treated P0s and four knock-ins were recovered from 36 F_1's laid by *cku-80* RNAi-treated P0 (Table 2).

For *nhr-23*::*2×FLAG* knock-in experiments, I used a knock-in-specific PCR screening approach; as in optimization experiments, it detected knock-in DNA diluted 1:1280 with WT DNA, whereas diagnostic restriction digestion of PCR products could only detect up to a 1:20 dilution of knock-in DNA with WT DNA (Figure S7). No knock-ins were recovered from 200 WT F_1 animals or 840 *lig-4* mutant F_1's (Table S8). In comparison, *pha-1(ts)* coselection using a similar sense *nhr-23*::*2×FLAG* repair template yielded seven knock-ins from 27 screened *pha-1(ts)* rescued F_1's (Figure 4C). Comparing all similar *nhr-23*::*2×FLAG* and *nhr-25*::*2×FLAG* direct selection and *pha-1* co-conversion experiments (*i.e.*, excluding antisense oligo and NHEJ inactivation experiments) demonstrated a significant increase in screening efficiency compared to direct F_1 screening (two-tailed *t*-test, $P = 0.01$).

Conclusions

Here, I demonstrate that selection for repair of a temperature-sensitive point mutation using an oligonucleotide template can be used to efficiently select for knock-in at other loci in as quickly as 8–9 days. Several findings of this work should be applicable for a range of co-conversion/co-CRISPR approaches.

First, the increased sgRNA(F+E) activity (Table 1) may improve knock-in and knock-out efficiencies and reduce the number of sgRNAs that one must test to identify an active sgRNA. Second, for introduction of single-basepair changes, efficient editing was observed using 60mers, 80mers, and 200mers. There may be a slight improvement in knock-in efficiency with longer repair templates, but using shorter oligos still produces repair events at a high rate. These data are consistent with the 29-bp repair track length observed using the second silent PAM mutation in the *nhr-23*::*2×FLAG* repair oligo and the efficient *nhr-23*::*2×FLAG* knock-ins obtained using 35 bp of homology (Figure 4). This optimal homology for oligo-mediated editing is similar to that reported for dsDNA templates (Paix *et al.* 2014). The 84-bp 3xFLAG *nhr-23* and *nhr-25* knock-ins is a larger insertion than described by several recent reports (Lo *et al.* 2013;

Arribere *et al.* 2014; Paix *et al.* 2014; Zhao *et al.* 2014); a 66-bp 3xFLAG insertion in the *nos-1* gene is the most comparable edit (Paix *et al.* 2014). Based on the minimal homology length of 35 bp and current oligo synthesis limit of 200 bp, it may be possible to knock in sequences of up to 130 bp using oligo templates. Third, I demonstrated that oligos do not need to be PAGE purified, as efficient editing was observed using unpurified 60mers and 200mers to edit the *pha-1(ts)* allele and to introduce the *nhr-23*::*2×FLAG* epitope (Figure 1D). However, PAGE purified oligos did result in increased knock-in efficiency and fewer imprecise knock-ins (Figure S6). Thus, an investigator can choose between the additional cost for the increased editing efficiency or simply inject more P0 animals and screen more F_1's. It is very important to note that there is likely wide variation in quality of unpurified oligos between different suppliers. Different preparations may contain different inhibitors or cytotoxic compounds and one should confirm the efficiency of unpurified oligos from a new supplier by testing a control such as *pha-1(ts)* rescue or *dpy-10(gf)* knock-in (Arribere *et al.* 2014). Fourth, PCR-generated P*U6*::*sgRNA* templates allow rapid production of new sgRNAs without need for cloning. Moreover, the robust sgRNA activity observed when injecting linear dsDNA templates enables other technologies for sgRNA template production such as gene synthesis or oligonucleotide arrays (Bassik *et al.* 2009; Gilbert *et al.* 2014), which could be used to create pooled sgRNA template libraries. Injecting multiple PCR-generated P*U6*::*sgRNA* templates allows several editing experiments to be performed simultaneously. From single-injection experiments, I was able to knock 3xFLAG tags into both the *nhr-23* and *nhr-25* loci or generate *2×FLAG*::*smo-1* lines while also determining that the *lig-4* sgRNAs were inactive (Table 2). Finally, the observation that inactivation of NHEJ can lead to improved knock-in rates can be adapted for any HR-based editing system, though it would reduce the efficiency of systems that rely on coselection of CRISPR-generated mutations as a marker. The increased knock-in efficiency observed following NHEJ inactivation was surprising and suggests that at least some knock-ins must be occurring outside in the germline; previous work has shown that NHEJ is actively suppressed in meiosis to ensure faithful repair of DSBs by homologous recombination (Adamo *et al.* 2010). Determining the cell types in which knock-ins are occurring and the DNA repair pathways involved could lead to improvements in editing efficiency.

It was intriguing that, for *pha-1* and *nhr-23*, higher editing efficiency was observed using oligos with homology to the coding strand. In these experiments, the sgRNA for *pha-1* recognized the coding strand, while the *nhr-23* PAM no. 1 sgRNA recognized the template strand (Figure 1D, Table S9). Although numerous explanations could be invoked for a polarity bias (sgRNA sequestration of the oligo, oligo:mRNA hybridization, different secondary structures in a given oligo and its reverse complement, etc.), it is unclear whether my data reflect a biologically meaningful trend or a chance observation. Best practice should be to clearly report the strand to which the sgRNA binds and the strand to which the oligo contains homologous sequence (Table S9). A metaanalysis of many more combinations of sgRNAs and oligos of differing polarities at a large number of genes is required to definitively determine whether oligo polarity is an important parameter. If one fails to obtain oligo-templated knock-ins when using a sgRNA with confirmed activity, then it may be worth testing the complement of the oligo.

The *pha-1(ts)* approach is distinct from reported co-CRISPR and co-conversion methods (Arribere *et al.* 2014; Kim *et al.* 2014) in that it starts with a mutant animal and results in restoration of a wild-type animal. In contrast, the other two approaches can be used with any strain, but require outcrossing or meiotic segregation of the selection marker. *pha-1(ts)* co-conversion may be advantageous as a marker in cases where the desired insertion site is linked to the selectable marker site. Arribere *et al.* (2014) demonstrated iterative editing using *dpy-10(gf)* co-conversion. *pha-1(ts)* co-conversion should allow for iterative editing events, though not as elegantly as the Arribere approach. *pha-1(ts)* F_1 rescues have all been heterozygous for the repair event. By shifting to the permissive temperature (15°) after generating homozygous animals of a desired knock-in, one could reisolate the *pha-1(ts)* allele and perform another round of editing; this *pha-1(ts)* reisolation would require an additional 5 days. Alternatively, one could simply cross the *pha-1(ts)* allele back into an edited strain.

The optimizations I report make oligo-mediated editing efficient, cost effective, and can be applicable to any CRISPR-mediated editing system. The development of three distinct variations of coediting selection (*unc-22* mutation; Kim *et al.* 2014), *rol-6(gf)/sqt-1(gf)/dpy-10(gf)* knock-in (Arribere *et al.* 2014), and *pha-1(ts)* repair (this article) highlight the robustness of this method to select for genome editing events. The recent description of PCR-derived dsDNA templates (Paix *et al.* 2014) will make these approaches even more powerful; the abundance of potential genetic markers in other model organisms should make these widely applicable approaches. A current challenge in cell-culture-based systems has been the laborious recovery of rare knock-in events. Coselection markers such as oligo-mediated repair of mutated GFP or drug resistance cassettes, or inactivation of hypoxanthine phosphoribosyl transferase, could yield similar improvements in editing event recovery in these systems.

Acknowledgments

I thank Teresita Bernal, Soledad de Guzman, and Greg Wright for experimental assistance; Dan Dickinson, Te-Wen Lo, Barbara Meyer, Rob Nakamura, Axel Bethke, and members of the Yamamoto lab for helpful discussions and technical advice; Lindsey Pack, Gabriela Monsalve, Debbie Thurtle, Elizabeth Silva, Stefan Taubert, Kaveh Ashrafi, and Keith Yamamoto for advice and comments on the manuscript; and the reviewers for their many excellent comments and experimental suggestions. Some strains were provided by the CGC, which is funded by National Institutes of Health

(NIH) Office of Research Infrastructure Programs (P40 OD010440). J.D.W. was supported by the National Institute Of General Medical Sciences of the NIH under award no. K99GM107345. Additional support was from NIH (CA20535) and U.S. National Science Foundation (MCB 1157767) awards to K. Yamamoto. The content is solely the responsibility of the author and does not necessarily represent the official views of the NIH.

Literature Cited

Adamo, A., S. J. Collis, C. A. Adelman, N. Silva, Z. Horejsi *et al.*, 2010 Preventing nonhomologous end joining suppresses DNA repair defects of Fanconi anemia. Mol. Cell 39: 25–35.

Arribere, J. A., R. T. Bell, B. X. H. Fu, K. L. Artiles, P. S. Hartman *et al.*, 2014 Efficient marker-free recovery of custom genetic modifications with CRISPR/Cas9 in *Caenorhabditis elegans*. Genetics 198: 837–846.

Asahina, M., T. Ishihara, M. Jindra, Y. Kohara, I. Katsura *et al.*, 2000 The conserved nuclear receptor Ftz-F1 is required for embryogenesis, moulting and reproduction in *Caenorhabditis elegans*. Genes Cells 5: 711–723.

Asahina, M., T. Valenta, M. Silhánková, V. Korinek, and M. Jindra, 2006 Crosstalk between a nuclear receptor and beta-catenin signaling decides cell fates in the *C. elegans* somatic gonad. Dev. Cell 11: 203–211.

Bassik, M. C., R. J. Lebbink, L. S. Churchman, N. T. Ingolia, W. Patena *et al.*, 2009 Rapid creation and quantitative monitoring of high coverage shRNA libraries. Nat. Methods 6: 443–445.

Bedell, V. M., Y. Wang, J. M. Campbell, T. L. Poshusta, C. G. Starker *et al.*, 2012 *In vivo* genome editing using a high-efficiency TALEN system. Nature 490: 114–118.

Beumer, K. J., J. K. Trautman, A. Bozas, J.-L. Liu, J. Rutter *et al.*, 2008 Efficient gene targeting in *Drosophila* by direct embryo injection with zinc-finger nucleases. Proc. Natl. Acad. Sci. USA 105: 19821–19826.

Bottcher, R., M. Hollmann, K. Merk, V. Nitschko, C. Obermaier *et al.*, 2014 Efficient chromosomal gene modification with CRISPR/cas9 and PCR-based homologous recombination donors in cultured *Drosophila* cells. Nucleic Acids Res. 42: e89.

Brenner, S., 1974 The genetics of *Caenorhabditis elegans*. Genetics 77: 71–94.

Broday, L., I. Kolotuev, C. Didier, A. Bhoumik, B. P. Gupta *et al.*, 2004 The small ubiquitin-like modifier (SUMO) is required for gonadal and uterine-vulval morphogenesis in *Caenorhabditis elegans*. Genes Dev. 18: 2380–2391.

Brooks, D. R., P. J. Appleford, L. Murray, and R. E. Isaac, 2003 An essential role in molting and morphogenesis of *Caenorhabditis elegans* for ACN-1, a novel member of the angiotensin-converting enzyme family that lacks a metallopeptidase active site. J. Biol. Chem. 278: 52340–52346.

Chen, B., L. A. Gilbert, B. A. Cimini, J. Schnitzbauer, W. Zhang *et al.*, 2013a Dynamic imaging of genomic loci in living human cells by an optimized CRISPR/Cas system. Cell 155: 1479–1491.

Chen, C., L. A. Fenk, and M. de Bono, 2013b Efficient genome editing in *Caenorhabditis elegans* by CRISPR-targeted homologous recombination. Nucleic Acids Res. 41: e193.

Chen, F., S. M. Pruett-Miller, Y. Huang, M. Gjoka, K. Duda *et al.*, 2011 High-frequency genome editing using ssDNA oligonucleotides with zinc-finger nucleases. Nat. Methods 8: 753–755.

Chen, Z., D. J. Eastburn, and M. Han, 2004 The *Caenorhabditis elegans* nuclear receptor gene *nhr-25* regulates epidermal cell development. Mol. Cell. Biol. 24: 7345–7358.

Chiu, H., H. T. Schwartz, I. Antoshechkin, and P. W. Sternberg, 2013 Transgene-free genome editing in *Caenorhabditis elegans* using CRISPR-Cas. Genetics 195: 1167–1171.

Cho, S. W., J. Lee, D. Carroll, J.-S. Kim, and J. Lee, 2013 Heritable gene knockout in *Caenorhabditis elegans* by direct injection of Cas9-sgRNA ribonucleoproteins. Genetics 195: 1177–1180.

Clejan, I., J. Boerckel, and S. Ahmed, 2006 Developmental modulation of nonhomologous end joining in *Caenorhabditis elegans*. Genetics 173: 1301–1317.

Cong, L., F. A. Ran, D. Cox, S. Lin, R. Barretto *et al.*, 2013 Multiplex genome engineering using CRISPR/Cas systems. Science 339: 819–823.

DiCarlo, J. E., J. E. Norville, P. Mali, X. Rios, J. Aach *et al.*, 2013 Genome engineering in *Saccharomyces cerevisiae* using CRISPR-Cas systems. Nucleic Acids Res. 41: 4336–4343.

Dickinson, D. J., J. D. Ward, D. J. Reiner, and B. Goldstein, 2013 Engineering the *Caenorhabditis elegans* genome using Cas9-triggered homologous recombination. Nat. Methods 10: 1028–1034.

Dmitrieva, N. I., A. Celeste, A. Nussenzweig, and M. B. Burg, 2005 Ku86 preserves chromatin integrity in cells adapted to high NaCl. Proc. Natl. Acad. Sci. USA 102: 10730–10735.

Friedland, A. E., Y. B. Tzur, K. M. Esvelt, M. P. Colaiácovo, G. M. Church *et al.*, 2013 Heritable genome editing in *C. elegans* via a CRISPR-Cas9 system. Nat. Methods 10: 741–743.

Frøkjaer-Jensen, C., M. W. Davis, C. E. Hopkins, B. J. Newman, J. M. Thummel *et al.*, 2008 Single-copy insertion of transgenes in *Caenorhabditis elegans*. Nat. Genet. 40: 1375–1383.

Frøkjær-Jensen, C., M. W. Davis, G. Hollopeter, J. Taylor, T. W. Harris *et al.*, 2010 Targeted gene deletions in *C. elegans* using transposon excision. Nat. Methods 7: 451–453.

Frøkjær-Jensen, C., M. W. Davis, M. Ailion, and E. M. Jorgensen, 2012 Improved Mos1-mediated transgenesis in *C. elegans*. Nat. Methods 9: 117–118.

Gilbert, L. A., M. A. Horlbeck, B. Adamson, J. E. Villalta, Y. Chen *et al.*, 2014 Genome-scale CRISPR-mediated control of gene repression and activation. Cell 159: 647–661.

Giordano-Santini, R., S. Milstein, N. Svrzikapa, D. Tu, R. Johnsen *et al.*, 2010 An antibiotic selection marker for nematode transgenesis. Nat. Methods 7: 721–723.

Gissendanner, C. R., and A. E. Sluder, 2000 *nhr-25*, the *Caenorhabditis elegans* ortholog of *ftz-f1*, is required for epidermal and somatic gonad development. Dev. Biol. 221: 259–272.

Granato, M., H. Schnabel, and R. Schnabel, 1994 *pha-1*, a selectable marker for gene transfer in *C. elegans*. Nucleic Acids Res. 22: 1762–1763.

Gratz, S. J., A. M. Cummings, J. N. Nguyen, D. C. Hamm, L. K. Donohue *et al.*, 2013 Genome engineering of *Drosophila* with the CRISPR RNA-guided Cas9 nuclease. Genetics 194: 1029–1035.

Gratz, S. J., F. P. Ukken, C. D. Rubinstein, G. Thiede, L. K. Donohue *et al.*, 2014 Highly specific and efficient CRISPR/Cas9-catalyzed homology-directed repair in *Drosophila*. Genetics 196: 961–971.

Hobert, O., 2002 PCR fusion-based approach to create reporter gene constructs for expression analysis in transgenic *C. elegans*. Biotechniques 32: 728–730.

Hwang, W. Y., Y. Fu, D. Reyon, M. L. Maeder, S. Q. Tsai *et al.*, 2013 Efficient genome editing in zebrafish using a CRISPR-Cas system. Nat. Biotechnol. 31: 227–229.

Igoucheva, O., V. Alexeev, and K. Yoon, 2001 Targeted gene correction by small single-stranded oligonucleotides in mammalian cells. Gene Ther. 8: 391–399.

Jinek, M., K. Chylinski, I. Fonfara, M. Hauer, J. A. Doudna *et al.*, 2012 A programmable dual-RNA-guided DNA endonuclease in adaptive bacterial immunity. Science 337: 816–821.

Kamath, R. S., A. G. Fraser, Y. Dong, G. Poulin, R. Durbin *et al.*, 2003 Systematic functional analysis of the *Caenorhabditis elegans* genome using RNAi. Nature 421: 231–237.

Kamath R. S., M. Martinez-Campos, P. Zipperlen, A. G. Fraser, and J. Ahringer, 2001 Effectiveness of specific RNA-mediated interference through ingested double-stranded RNA in *Caenorhabditis elegans*. Genome Biol 2: RESEARCH0002.

Kaminsky, R., C. Denison, U. Bening-Abu-Shach, A. D. Chisholm, S. P. Gygi *et al.*, 2009 SUMO regulates the assembly and function of a cytoplasmic intermediate filament protein in *C. elegans*. Dev. Cell 17: 724–735.

Katic, I., and H. Grosshans, 2013 Targeted heritable mutation and gene conversion by Cas9-CRISPR in *Caenorhabditis elegans*. Genetics 195: 1173–1176.

Kim, H., T. Ishidate, K. S. Ghanta, M. Seth, D. Conte *et al.*, 2014 A Co-CRISPR strategy for efficient genome editing in *Caenorhabditis elegans*. Genetics 197: 1069–1080.

Kostrouchova, M., M. Krause, Z. Kostrouch, and J. E. Rall, 1998 CHR3: a *Caenorhabditis elegans* orphan nuclear hormone receptor required for proper epidermal development and molting. Development 125: 1617–1626.

Kostrouchova, M., M. Krause, Z. Kostrouch, and J. E. Rall, 2001 Nuclear hormone receptor CHR3 is a critical regulator of all four larval molts of the nematode *Caenorhabditis elegans*. Proc. Natl. Acad. Sci. USA 98: 7360–7365.

Li, J.-F., J. E. Norville, J. Aach, M. McCormack, D. Zhang *et al.*, 2013 Multiplex and homologous recombination-mediated genome editing in *Arabidopsis* and *Nicotiana* benthamiana using guide RNA and Cas9. Nat. Biotechnol. 31: 688–691.

Lo, T.-W., C. S. Pickle, S. Lin, E. J. Ralston, M. Gurling *et al.*, 2013 Precise and heritable genome editing in evolutionarily diverse nematodes using TALENs and CRISPR/Cas9 to engineer insertions and deletions. Genetics 195: 331–348.

Mali, P., K. M. Esvelt, and G. M. Church, 2013 Cas9 as a versatile tool for engineering biology. Nat. Methods 10: 957–963.

McColl, G., M. C. Vantipalli, and G. J. Lithgow, 2005 The *C. elegans* ortholog of mammalian Ku70, interacts with insulin-like signaling to modulate stress resistance and life span. FASEB J. 19: 1716–1718.

Moerman, D. G., and D. L. Baillie, 1979 Genetic organization in *Caenorhabditis elegans*: fine-structure analysis of the *unc-22* gene. Genetics 91: 95–103.

Mullaney, B. C., R. D. Blind, G. A. Lemieux, C. L. Perez, I. C. Elle *et al.*, 2010 Regulation of *C. elegans* fat uptake and storage by acyl-CoA synthase-3 is dependent on NR5A family nuclear hormone receptor *nhr-25*. Cell Metab. 12: 398–410.

Nakanishi, T., Y. Kato, T. Matsuura, and H. Watanabe, 2014 CRISPR/Cas-mediated targeted mutagenesis in *Daphnia magna*. PLoS ONE 9: e98363.

Paix, A., Y. Wang, H. E. Smith, C.-Y. S. Lee, D. Calidas *et al.*, 2014 Scalable and versatile genome editing using linear DNAs with microhomology to Cas9 sites in *Caenorhabditis elegans*. Genetics 198: 1347–1356.

Plasterk, R. H., and J. T. Groenen, 1992 Targeted alterations of the *Caenorhabditis elegans* genome by transgene instructed DNA double strand break repair following Tc1 excision. EMBO J. 11: 287–290.

Posch, A., J. Kohn, K. Oh, M. Hammond, and N. Liu, 2013 V3 stain-free workflow for a practical, convenient, and reliable total protein loading control in western blotting. J. Vis. Exp. 30: 50948.

Ran, F. A., P. D. Hsu, J. Wright, V. Agarwala, D. A. Scott *et al.*, 2013 Genome engineering using the CRISPR-Cas9 system. Nat. Protoc. 8: 2281–2308.

Robert, V., and J.-L. Bessereau, 2007 Targeted engineering of the *Caenorhabditis elegans* genome following Mos1-triggered chromosomal breaks. EMBO J. 26: 170–183.

Schnabel, H., G. Bauer, and R. Schnabel, 1991 Suppressors of the organ-specific differentiation gene *pha-1* of *Caenorhabditis elegans*. Genetics 129: 69–77.

Shtonda, B. B., and L. Avery, 2006 Dietary choice behavior in *Caenorhabditis elegans*. J. Exp. Biol. 209: 89–102.

Storici, F., C. L. Durham, D. A. Gordenin, and M. A. Resnick, 2003 Chromosomal site-specific double-strand breaks are efficiently targeted for repair by oligonucleotides in yeast. Proc. Natl. Acad. Sci. USA 100: 14994–14999.

Tzur, Y. B., A. E. Friedland, S. Nadarajan, G. M. Church, J. A. Calarco *et al.*, 2013 Heritable custom genomic modifications in *Caenorhabditis elegans* via a CRISPR-Cas9 system. Genetics 195: 1181–1185.

Waaijers, S., and M. Boxem, 2014 Engineering the *Caenorhabditis elegans* genome with CRISPR/Cas9. Methods 68: 381–388.

Waaijers, S., V. Portegijs, J. Kerver, B. B. L. G. Lemmens, M. Tijsterman *et al.*, 2013 CRISPR/Cas9-targeted mutagenesis in *Caenorhabditis elegans*. Genetics 195: 1187–1191.

Ward, J. D., N. Bojanala, T. Bernal, K. Ashrafi, M. Asahina *et al.*, 2013 Sumoylated NHR-25/NR5A regulates cell fate during *C. elegans* vulval development. PLoS Genet. 9: e1003992.

Ward, J. D., B. Mullaney, B. J. Schiller, L. D. He, S. E. Petnic *et al.*, 2014 Defects in the *C. elegans* acyl-CoA synthase, *acs-3*, and nuclear hormone receptor, *nhr-25*, cause sensitivity to distinct, but overlapping stresses. PLoS ONE 9: e92552.

Wood, A. J., T.-W. Lo, B. Zeitler, C. S. Pickle, E. J. Ralston *et al.*, 2011 Targeted genome editing across species using ZFNs and TALENs. Science 333: 307.

Yang, B., X. Wen, N. S. Kodali, C. A. Oleykowski, C. G. Miller *et al.*, 2000 Purification, cloning, and characterization of the CEL I nuclease. Biochemistry 39: 3533–3541.

Zhao, P., Z. Zhang, H. Ke, Y. Yue, and D. Xue, 2014 Oligonucleotide-based targeted gene editing in *C. elegans* via the CRISPR/Cas9 system. Cell Res. 24: 247–250.

Communicating editor: O. Hobert

GENETICS

Supporting Information
http://www.genetics.org/lookup/suppl/doi:10.1534/genetics.114.172361/-/DC1

Rapid and Precise Engineering of the *Caenorhabditis elegans* Genome with Lethal Mutation Co-Conversion and Inactivation of NHEJ Repair

Jordan D. Ward

DOI: 10.1534/genetics.114.172361

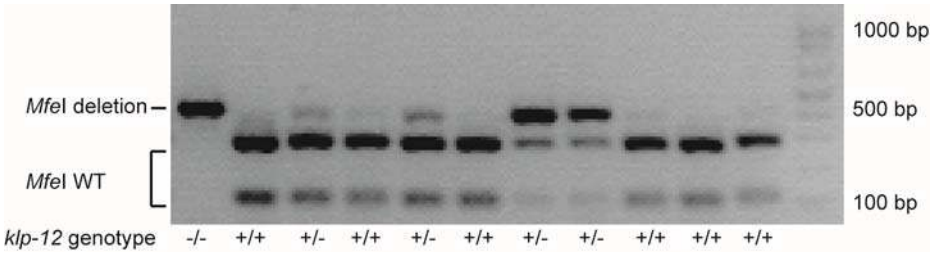

Figure S1 Representative *klp-12* deletion experiment. Injection of 50 ng/µl of CRISPR/Cas9 plasmid targeting a previously described PAM in the *klp-12* locus (FRIEDLAND *et al.* 2013) results in deletion of an adjacent *Mfe*I restriction site. WT and mutated *Mfe*I digested PCR products are indicated. Products were run on a 1.5% TAE-agarose gel and the 1KB+ (Invitrogen) size standard is provided. *klp-12* genotype inferred by *Mfe*I digestion is indicated. WT animals have complete *Mfe*I digestion of the PCR product, mutant homozygotes have no digestion of the PCR product, and heterozygotes have a mixture of digested and undigested PCR products.

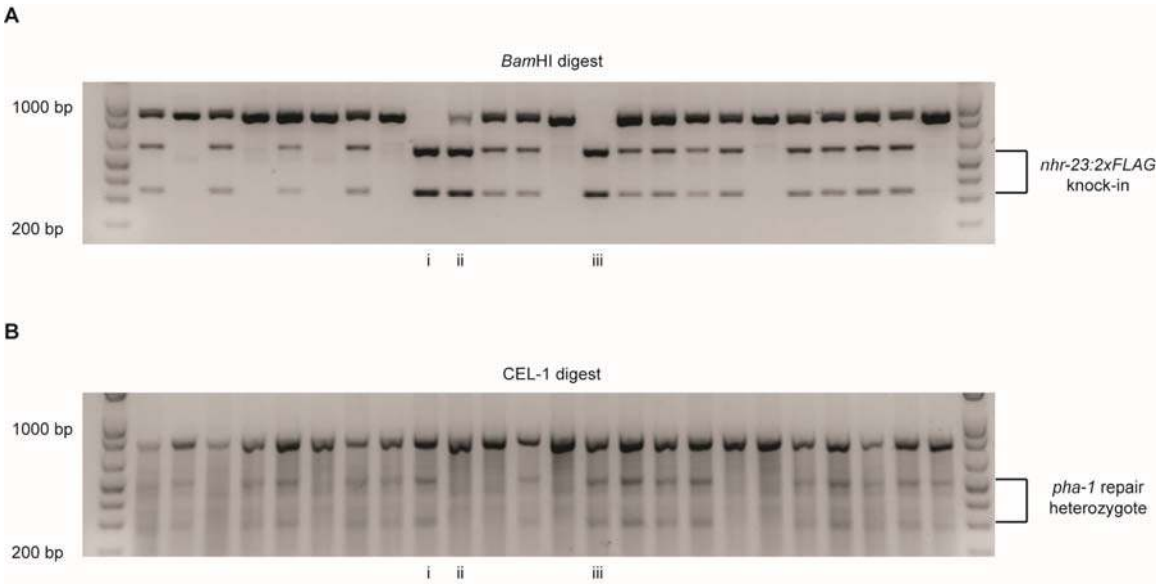

Figure S2 Representative genotyping of the progeny of an *nhr-23::2xFLAG* knock-in heterozygote. (A) *Bam*HI digestion to genotype *nhr-23::2xFLAG* knock-in. Twenty-four progeny from an *nhr-23::2xFLAG* knock-in heterozygote were plated out, allowed to lay progeny, and the parental animal was genotyped. Candidate homozygotes are indicated by i, ii, and iii. (B) CEL-1 digestion of PCR products amplifying the *pha-1(ts)* repair site. CEL-1 cuts mismatches. (i and iii) are *pha-1* repair heterozygotes, as indicated by the digestion product. (ii) is a *pha-1(ts)* repair homozygote. *pha-1* and *nhr-23::2xFLAG* genotypes were confirmed by sequencing of the PCR products. The 1KB+ (Invitrogen) size standard is provided in A and B.

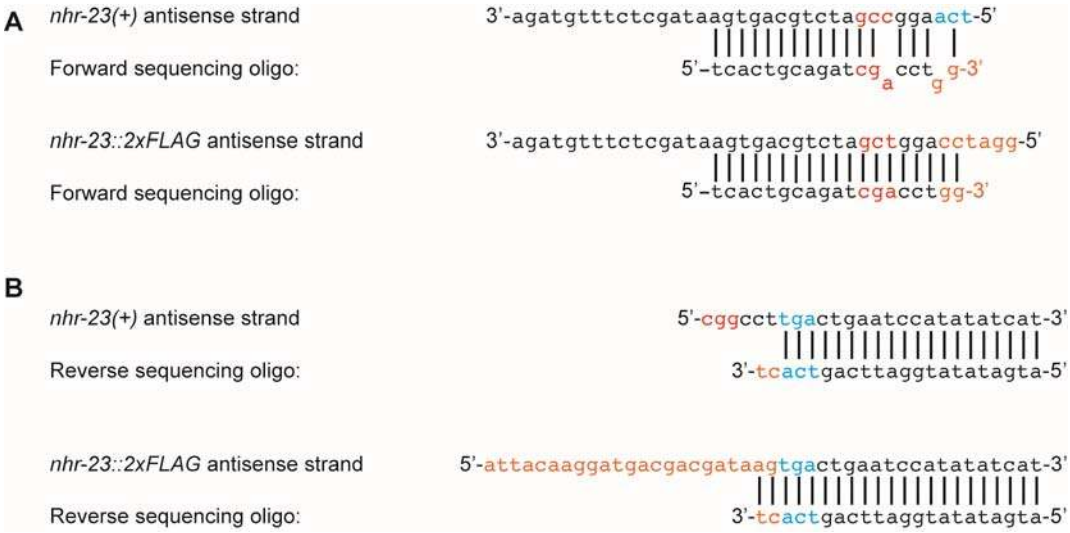

Figure S3 Oligo design to sequence FLAG knock-in heterozygotes. Design of oligos to sequence into 5' end (A) and 3' end (B) of *nhr-23* 2x and 3x FLAG knock-ins. The non-coding strand of *nhr-23 (+)* is shown paired with the sequencing oligo. The stop codon (blue text), PAM #1 (red text), and a portion of the 2xFLAG knock-in sequence (orange text) are indicated. The oligo is designed to bind the genomic sequence at the insertion site with the last two bases binding bases in the insert. In cases where sequence is too poor to confirm correct insertion of an epitope, an additional round of PCR can be performed using one of the insert-specific oligos and an external primer that binds in the genomic sequence. Purification of this product followed by sequencing using the primer that binds in the genomic sequence provides the entire epitope sequence. In events where 2 bp of knock-in sequence is not sufficient to confer specificity, increasing the knock-in specific homology will correct the problem at the expense of sequencing coverage of the knock-in.

A

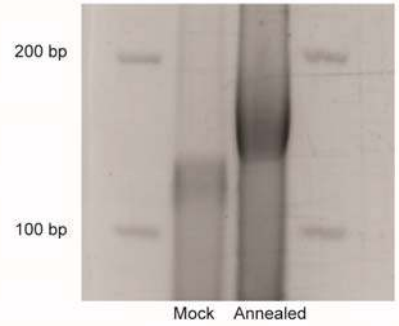

B

nhr-23::2xFLAG oligo	Viable injected P0	Rescued F1	P0 with rescued F1	PCR hits	Precise Knockins	% Knockins/ rescued F1	% Knockins/ P0
sense 200mer	102	27	n/a	10	7	25.9	6.9
sense 200mer mock annealed	20	5	2	3	1	20.0	5.0
sense+antisense 200mer mock annealed	32	9	2	1	1	11.1	3.1
sense+antisense 200mer annealed	24	4	4	0	0	0.0	0.0

Figure S4 dsDNA is not a more effective template than ssDNA for introduction of a *2xFLAG* epitope at the 3' end of *nhr-23*. (A) 50 ng/µl of sense of and antisense *nhr-23::2xFLAG* oligos in annealing buffer (TE buffer with 50 mM NaCl) were either annealed by heating to 95ºC for two minutes and then slowly cooling to 25ºC over 30 minutes in a thermocycler, or mock annealed (kept at 25ºC). Annealing was confirmed by resolving the annealed and mock annealed oligos on a 4% TAE-agarose gel and staining with GelRed. The 1KB+ (Invitrogen) size standard is provided. (B) Table comparing the knock-in efficiencies of sense oligos, and either mock annealed or annealed sense+antisense *nhr-23::2xFLAG* 200mers. The sense 200mer data is pooled from all experiments using *pha-1(ts)* sense oligos and *nhr-23::2xFLAG* sense 200mers (Figures 1 and 3). A control where the sense oligo was injected in annealing buffer was performed to ensure that the buffer did not affect knock-in efficiency.

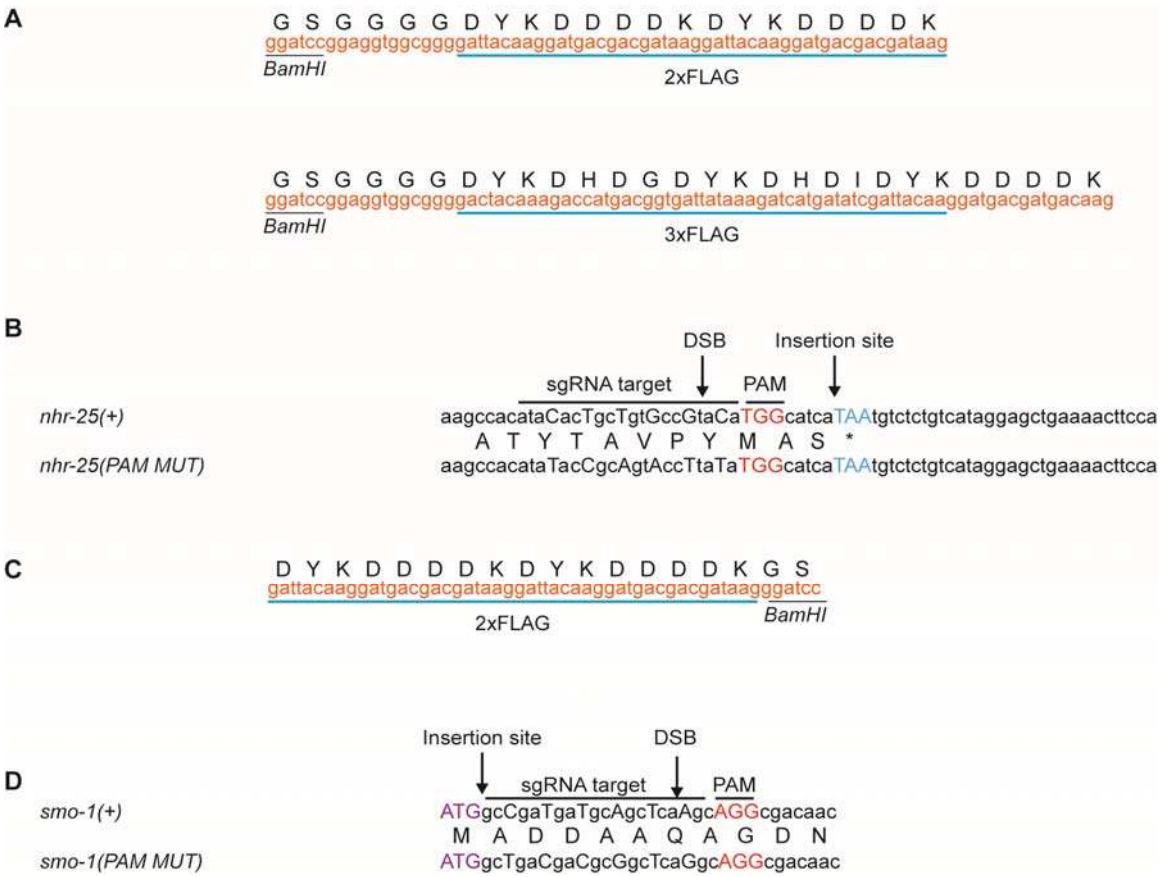

Figure S5 FLAG tag sequences and schematic of insertion sites in *nhr-25* and *smo-1*. (A) DNA and amino acid sequence of 2x and 3x FLAG epitopes used in *nhr-23* and *nhr-25* editing experiments. A GSGGGG amino acid linker sequence precedes the epitope; a *Bam*HI site is encoded in this linker sequence for genotyping by restriction digestion. (B) Sequence of the *nhr-25* genomic locus targeted. The PAM (red text), sgRNA target sequence, stop codon (blue text), and position of the DSB are indicated. The amino acid sequence of the targeted locus is provided. The bases mutated in the oligo template to inactivate the PAM (*nhr-25(PAM MUT)* are in uppercase font in the sgRNA target sequence, with the corresponding WT bases in *nhr-25(+).* (C) DNA and amino acid sequence of the 2x FLAG epitope used in *smo-1* editing experiments. A glycine-serine dipeptide linker encoding a *Bam*HI site for diagnostic restriction digestion follows the epitope. (D) Sequence of the *smo-1* genomic locus targeted. The PAM (red text), sgRNA target sequence, start codon (purple text), and position of the DSB are indicated. The amino acid sequence of the targeted locus is provided. The bases mutated in the oligo template to inactivate the PAM (*smo-1(PAM MUT)* are in uppercase font in the sgRNA target sequence, with the corresponding WT bases in *smo-1(+).*

A

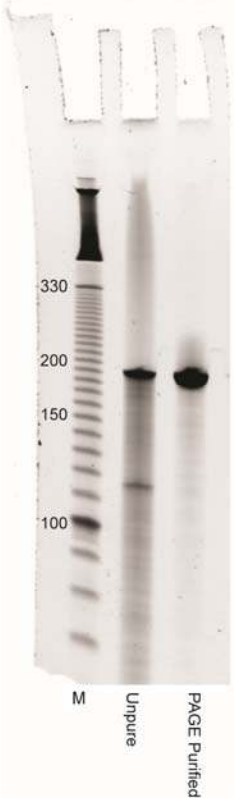

B

P0 strain	Oligo	Succesfully injected P0	F1 screened	PCR hits	Precise Knockins	% Knockins per F1	% Knockins per P0
pha-1(ts); control(RNAi)	Unpure	8	3	0	0	0.0	0.0
pha-1(ts); cku-80(RNAi)	Unpure	25	11	1	1	9.1	4.0
pha-1(ts); control(RNAi)	PAGE pure	11	3	1	1	33.3	9.1
pha-1(ts); cku-80(RNAi)	PAGE pure	7	2	1	1	50.0	14.3

C

Oligo	Succesfully injected P0	F1 screened	PCR hits	Precise Knockins	% Knockins per F1	% Knockins per P0
Unpure	80	26	4	2	7.7	2.5
PAGE pure	18	5	2	2	40.0	11.1

Figure S6 PAGE purification of oligos results in increased knock-in efficiency. (A) Comparison of PAGE purified and unpurified *nhr-25::3xFLAG* oligos. 200 ng of oligos were resolved on a denaturing 8% TBE-Urea polyacrylamide gel and stained with SYBR Gold. A 100 bp ladder (Invitrogen; sizes in bp) is provided as a standard. (B) Comparison of knock-in efficiency of unpurified and PAGE purified oligos in animals grown on HB101 and then transferred to either control RNAi or *cku-80* RNAi. (C) Comparison of all experiments using unpurified vs PAGE purified *nhr-25::3xFLAG* oligos.

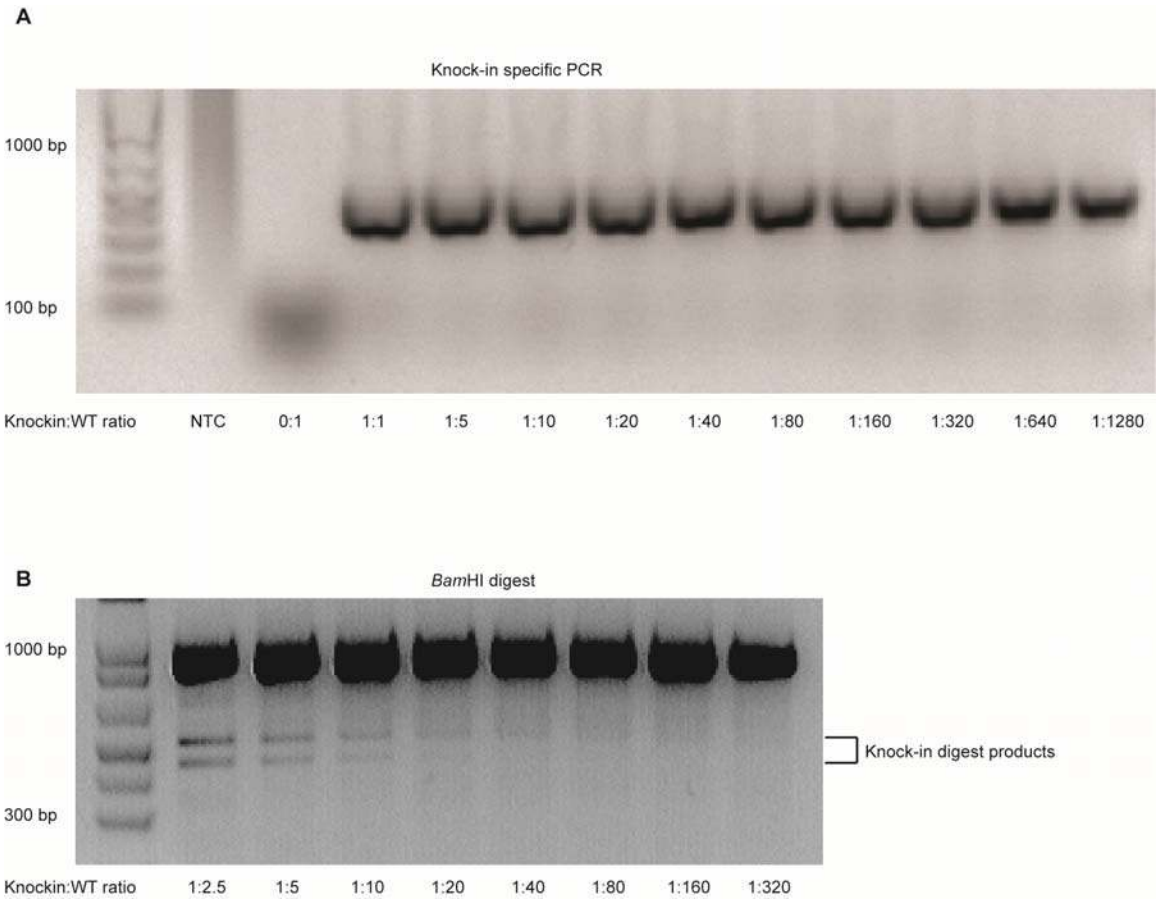

Figure S7 Detection of knock-ins by knock-in specific PCR and diagnostic restriction digestion. (A) For *nhr::23::2xFLAG* direct screening, a knock-in specific PCR approach was developed to minimize the number of PCRs required to identify knock-ins. Using the *nhr-25::2xFLAG* strain generated by direct selection (Table S8) as a control, oligos were designed to bind within the inserted sequence (oligo #1715) and outside of the insertion area. *nhr-25::2xFLAG* knock-in lysate was diluted as indicated with WT lysate and used as template in a knock-in specific genotyping PCR. No product was detected in the absence of *nhr-25::2xFLAG* lysate and knock-in product could be detected across the dilution range, to 1:1280. (NTC; no template control). (B) Identification of *nhr-25:2xFLAG* knock-in by diagnostic restriction digest. *nhr-25::2xFLAG* lysate was diluted and used in genotyping PCR as in (A). The product was then digested by *Bam*HI to detect knock-ins. Knock-in product could be detected up to a 1:20 dilution. The 1KB+ (Invitrogen) size standard is provided in A and B.

File S1
Supplemental Methods

PCR-based knock-in screening

For direct screening of *nhr-25::2xFLAG* knock-ins, WT animals or *lig-4(ok716)* mutants were injected with 100 ng/µl of pJW1185 (*nhr-25* targeting CRISPR/Cas9), 10 ng/µl of a *myo-2::tdTomato* co-injection marker, and 100 ng/µl of a *nhr-25::2xFLAG* 135 mer (oligo #1580, Table S2). P0 animals were plated in single wells of 12-well plates containing NGM-lite agar seeded with OP50 *E. coli*. Following incubation at 25ºC for three days, wells were scored for the presence of marker positive F1 progeny. From these wells, the marker positive F1 were picked off and discarded and 1 ml of M9+gelatin was added. This step was performed because previous reports suggested that edits occurred in marker negative F1 (ZHAO *et al.* 2014). Marker negative F1s from these wells were pipetted into 30 µl of M9+gelatin in a 96-well plate; four worms were pipetted into each well. A multichannel pipette was used to add 30 µl of 2xOP50 food to each well. This food was made by inoculating a one liter culture of LB+streptomycin (50 µg/ml) with a single colony of OP50, shaking for 16 hours at 225 rpm at 37ºC, pelleting the culture by spinning at 4000 rpm, and resuspending in 10 ml of M9. For the 2xOP50 food, 5 ml of this concentrated OP50 was added to 45 ml of M9+gelatin containing 10 µg/ml cholesterol. Plates were parafilmed and incubated at 25ºC for 3-4 days. Lysates were made by using a multichannel pipette to transfer 10 µl of worm culture to 10 µl of single-worm lysis buffer containing proteinase K in a 96-well plate. The lysates were then processed, and genotyping PCRs and BamHI digests performed as described in the "Genotyping PCRs and restriction digestion" section in the main-text Methods. For wells with a hit, in order to identify homozygotes, 24 F2 progeny were transferred to single wells of a 96-well plate and incubated and screened as above.

For pooled screening of *nhr-23::2xFLAG* knock-ins, WT animals or *lig-4(ok716)* mutants were injected with 50 ng/µl of pJW1254 (*nhr-23* PAM #1 targeting CRISPR/Cas9), 5 ng/µl of a *myo-2::tdTomato* co-injection marker, and 50 ng/µl of a sense *nhr-23::2xFLAG* 199mer (oligo #1719, Table S2). P0 animals were plated and marker positive wells were identified as above. All progeny from marker positive wells were washed out with 1 ml of M9+gelatin and diluted to ~10 worms/30µl and this volume (30 µl) was plated in 96 wells using a repeat pipetter. The number of worms/well was averaged in two rows of the plate to confirm the estimated concentration of 10 worms/well. Food was added, the plates were incubated, and lysates made as described above. Knock-in specific PCRs were performed using an oligo that internally bound the *2xFLAG* sequence (#1715) and an oligo that bound external to the knock-in sequence. Four rows were pooled for each PCR reaction with 0.5 µl of lysate from each row used in a 20 µl PCR. For wells with a hit, in order to identify homozygotes, 48-96 F2 progeny were transferred to single wells of a 96-well plate and incubated and screened as above.

Generation of lysates for immunoblotting

For the immunoblot in Figure 2, animals of the indicated genotype were synchronized by alkaline bleaching followed by plating overnight in the absence of food. Approximately 3000 arrested L1s were plated on 10 cm NGM-lite plates seeded with OP50 and incubated at 25ºC for 48 hours, at which point the animals were gravid adults. Animals were washed off of the plates with M9+gelatin, pelleted and transferred to a 1.5 ml tube and washed four times with 1 ml

of M9. The M9 was aspirated, leaving 150 µl and the pellet flash-frozen in liquid nitrogen and stored at -80ºC. The pellet was resuspended by adding 150 µl 2xRIPA buffer (100 mM Tris-HCl, 900 mM NaCl, 2% NP-40, 1% Sodium deoxycholate and 0.2% SDS, pH 7.4) supplemented with Protease Inhibitor Cocktail Set III, EDTA-free (Calbiochem, #539134-1SET), 1mM PMSF, 10 µM MG-132 proteasome inhibitor (Caymon, #10012628), and 1 mM DTT. Worms were lysed by three cycles of sonication on ice (10 sec, 20% amplitude). Debris was pelleted by centrifugation at 14,000 rpm for 10 minutes at 4ºC and protein concentration was determined by a 660nm Protein Assay (Pierce). Four micrograms of total protein was resolved by SDS-PAGE using a Mini-PROTEAN TGX Stain-Free 4-15% gradient gel (Bio-Rad, #456-8086).

For the immunoblot in Figure 5, ten gravid adults were placed on 10 cm plates and incubated for four days at 25ºC. Lysates were made by washing crowded, mixed stage animals off of these 10 cm plates in M9+gelatin, pelleting at 700xg for two minutes, and transferring to a 1.5 ml tube. The worms were washed four additional times with 1 ml of M9+gelatin. The M9+gelatin was aspirated to just above the worm pellet and the pellet was rapidly freeze-thawed three times (cycling between liquid nitrogen and a 42ºC water bath) before 4x Laemmli buffer was added to a final concentration of 1x. The samples boiled for 10 minutes, then the lysate was frozen for 15 minutes on dry ice and then boiled again for 10 minutes. Debris was pelleted by centrifugation at 14,000 rpm in a microcentrifuge for 5 minutes. Ten microlitres of lysate was resolved by SDS-PAGE on a Mini-PROTEAN TGX 4-15% gradient gel (Bio-Rad, catalog #456-1086) at run at 250 V.

PEG/DMSO DH5a competent cells

A single DH5 alpha colony from a freshly struck plate was used to inoculate a 5 ml LB culture and and incubated overnight at 37ºC shaking at 225 rpm. This culture was used to inoculate 500 ml of LB which was shaken at 37ºC until an OD600 of 0.5-0.6 was reached. Cells were pelleted by centrifugation for 5 min at 2000 rpm, 4ºC. Cells were gently resuspended in 25 ml of ice cold TSB buffer (LB pH 6.1, 10% PEG-3350, 5% DMSO, 10 mM $MgCl_2$, 10 mM $MGSO_4$), incubated on ice for 10 minutes, aliquoted, flash frozen in liquid nitrogen, and stored at -80ºC. To transform the cells, an aliquot was thawed on ice and the DNA to be transformed was mixed with 5xKCM (500 mM KCl, 150 mM $CaCl_2$, 250 mM $MgCl_2$) and dH20 to a final volume of 100 µl at 1xKCM final concentration. An equal amount of cells was added, mixed by gentle inversion, and incubated on ice for 20 minutes. The mixture was then incubated at room temperature for 10 minutes before 1 ml of SOC or LB was added and the transformation was shaken for 1 hr at 37ºC before plating on LB containing appropriate antibiotics.

Table S1 Strains generated for this study

Strain name	Genotype
KRY41	*lig-4(ok716)* III*; nhr-25(kry1[nhr-25::2xFLAG])* X
KRY42	*nhr-25(kry1[nhr-25::2xFLAG])* X
KRY46	*nhr-23(kry4[nhr-23::2xFLAG])* I*; pha-1(kry5[Y169C*e2123])* III
KRY47	*nhr-23(kry6[nhr-23::2xFLAG])* I*; pha-1(kry7[Y169C*e2123])* III
KRY48	*nhr-23(kry8[nhr-23::2xFLAG])* I*; pha-1(kry9[Y169C*e2123])* III
KRY49	*nhr-23(kry10[nhr-23::2xFLAG])* I*; pha-1(kry11[Y169C*e2123])* III
KRY50	*nhr-23(kry12[nhr-23::2xFLAG])* I*; pha-1(kry13[Y169C*e2123])* III
KRY51	*nhr-23(kry14[nhr-23::2xFLAG])* I*; pha-1(kry15[Y169C*e2123])* III
KRY52	*nhr-23(kry16[nhr-23::2xFLAG])* I*; pha-1(kry17[Y169C*e2123])* III
KRY53	*nhr-23(kry18[nhr-23::2xFLAG])* I*; pha-1(kry19[Y169C*e2123])* III
KRY54	*nhr-23(kry20[nhr-23::2xFLAG])* I*; pha-1(kry21[Y169C*e2123])* III
KRY55	*nhr-23(kry22[nhr-23::2xFLAG])* I*; pha-1(kry23[Y169C*e2123])* III
KRY56	*nhr-23(kry24[nhr-23::2xFLAG])* I*; pha-1(kry25[Y169C*e2123])* III
KRY57	*nhr-23(kry26[nhr-23::2xFLAG])* I*; pha-1(kry27[Y169C*e2123])* III
KRY58	*nhr-23(kry28[nhr-23::2xFLAG])* I*; pha-1(kry29[Y169C*e2123])* III
KRY59	*nhr-23(kry30[nhr-23::2xFLAG])* I*; pha-1(kry31[Y169C*e2123])* III
KRY60	*nhr-23(kry32[nhr-23::2xFLAG])* I*; pha-1(kry33[Y169C*e2123])* III
KRY64	*pha-1(kry34[Y169C*e2123])* III*; nhr-25(kry35[nhr-25::2xFLAG])* X
KRY65	*pha-1(kry36[Y169C*e2123])* III*; nhr-25(kry37[nhr-25::2xFLAG])* X
KRY66	*pha-1(kry38[Y169C*e2123])* III*; nhr-25(kry39[nhr-25::2xFLAG])* X
KRY67	*pha-1(kry40[Y169C*e2123])* III*; nhr-25(kry41[nhr-25::2xFLAG])* X
KRY70	*pha-1(kry42[Y169C*e2123])* III
KRY71	*pha-1(kry43[Y169C*e2123])* III
KRY72	*nhr-23(kry44[nhr-23::3xFLAG])* I*; pha-1(kry45[Y169C*e2123])* III
KRY73	*nhr-23(kry46[nhr-23::3xFLAG])* I*; pha-1(kry47[Y169C*e2123])* III
KRY74	*pha-1(kry48[Y169C*e2123])* III*; nhr-25(kry49[nhr-25::3xFLAG])* X
KRY75	*nhr-23(kry50[nhr-23::3xFLAG])* I*; pha-1(kry51[Y169C*e2123])* III*; nhr-25(kry52[nhr-25::3xFLAG])* X
KRY76	*nhr-23(kry6[nhr-23::2xFLAG])* I
KRY77	*nhr-23(kry44[nhr-23::3xFLAG])* I
KRY78	*nhr-23(kry50[nhr-23::3xFLAG])* I
KRY79	*nhr-25(kry35[nhr-25::2xFLAG])* X
KRY80	*nhr-25(kry52[nhr-25::3xFLAG])* X
KRY81	*smo-1(kry53[2xFLAG::smo-1]) I; pha-1(kry54[Y169C*e2123]) III*
KRY82	*smo-1(kry55[2xFLAG::smo-1]) I; pha-1(kry56[Y169C*e2123]) III*

Table S2 Repair oligos used for this study

Primer	Description	Sequence
1580	PAGE purified *nhr-25::2x FLAG* (sense 135mer)	aagccacatacactgctgtgccgtacatggcatcaggatccggaggtggcggggattacaaggatg acgacgataaggattacaaggatgacgacgataagtaatgtctctgtcataggagctgaaaacttc caa
1719	*nhr-23::2xFLAG* (sense 199mer; PAM #1 mutated)	tgtctgatccaacatcatctgaaaagcttcctgccctctacaaagagctattcactgcagatcgacct ggatccggaggtggcggggattacaaggatgacgacgataaggattacaaggatgacgacgata agtgactgaatccatatatcatcaatagttttatccatgctctccttccctatccccgtccatgaat
1831	*nhr-23::2xFLAG* (sense 200mer; PAM #1 and #2 mutated)	aaaacttccgaatgtctgatccaacatcatctgaaaagcttcctgcactctacaaagagctattcact gcagatcgacctggatccggaggtggcggggattacaaggatgacgacgataaggattacaagga tgacgacgataagtgactgaatccatatatcatcaatagttttatccatgctctccttccctatccc
1832	*nhr-23::2xFLAG* (antisense 200mer; PAM #1 and #2 mutated)	gggatagggaaggagagcatggataaaactattgatgatatatggattcagtcacttatcgtcgtca tccttgtaatccttatcgtcgtcatccttgtaatccccgccacctccggatccaggtcgatctgcagtg aatagctctttgtagagtgcaggaagcttttcagatgatgttggatcagacattcggaagtttt
1899	PAGE purified *pha-1* repair (sense 80mer)	caaaatacgaatcgaagactcaaaaagagtatgctgtatgattacagatgttcatcaagttattcat aaatcattgatag
1985	PAGE purified *pha-1* repair (antisense 80mer)	ctatcaatgatttatgaataacttgatgaacatctgtaatcatacagcatactctttttgagtcttcgat tcgtattttg
1986	*pha-1* repair (sense 60mer)	aatcgaagactcaaaaagagtatgctgtatgattacagatgttcatcaagttattcataa
1987	*pha-1* repair (sense 200mer)	ggagttttgttgtacattacatttcaggttcttaaaacaaaccatgaagattatggtaatcaaaatac gaatcgaagactcaaaaagagtatgctgtatgattacagatgttcatcaagttattcataaatcatt gataggttcagattgtaagtcttgattatctatcgttttgtaaagtgactaaactttaatcatta
1989	*nhr-25::2xFLAG* (sense 175mer; PAM mutated)	caggtcccagcaatccaactgccaaccccacaagccacatataccgcagtaccttatatggcatca ggatccggaggtggcggggattacaaggatgacgacgataaggattacaaggatgacgacgata agtaatgtctctgtcataggagctgaaaacttccaatggagtcag
2014	*nhr-25::3xFLAG* (sense 193mer; PAM mutated)	actcaggtcccagcaatccaactgccaaccccacaagccacatataccgcagtaccttatatggcat caggatccggaggtggcggggactacaaagaccatgacggtgattataaagatcatgatatcgatt acaaggatgacgatgacaagtaatgtctctgtcataggagctgaaaacttccaatggagt
2015	*nhr-23::3xFLAG* (sense 193mer; PAM #1 and #2 mutated)	ttccgaatgtctgatccaacatcatctgaaaagcttcctgcactctacaaagagctattcactgcaga tcgacctggatccggaggtggcggggactacaaagaccatgacggtgattataaagatcatgatat cgattacaaggatgacgatgacaagtgactgaatccatatatcatcaatagttttatccatgctc
2085	*nhr-25::3xFLAG* (sense 193mer; PAM mutated)-PAGE purified	actcaggtcccagcaatccaactgccaaccccacaagccacatataccgcagtaccttatatggcat caggatccggaggtggcggggactacaaagaccatgacggtgattataaagatcatgatatcgatt acaaggatgacgatgacaagtaatgtctctgtcataggagctgaaaacttccaatggagt

2086	*nhr-23::2xFLAG* (sense 140mer; 35 bp homology arms)	cctgccctctacaaagagctattcactgcagatcgacctggatccggaggtggcggggattacaag gatgacgacgataaggattacaaggatgacgacgataagtgactgaatccatatatcatcaatagt tttatcca
2087	*nhr-23::2xFLAG* (sense 120mer; 25 bp homology arms)	acaaagagctattcactgcagatcgacctggatccggaggtggcggggattacaaggatgacgac gataaggattacaaggatgacgacgataagtgactgaatccatatatcatcaata
2088	*nhr-23::2xFLAG* (sense 100mer; 15 bp homology arms)	attcactgcagatcgacctggatccggaggtggcggggattacaaggatgacgacgataaggatta caaggatgacgacgataagtgactgaatccatat
2089	*nhr-23::2xFLAG* (sense 200mer; PAM #1, #2, and #3 mutated)	aaaacttccgaatgtctgatccaacatcatctgaaaagcttcctgcactctacaaagagctattcact gcagatcgacctggatccggaggtggcggggattacaaggatgacgacgataaggattacaagga tgacgacgataagtgactgaatccatatatcatcaatagttttatccatgctctccttccctatccc
2099	*lig-4* (sense 60mer; insert stop codon, delete part of exon 1)	agtagttgacgtcttcaacaagatttaaggatccgtaagacaattgggcgaactattaca
2105	*2xFLAG::smo-1* (sense 175mer; PAM mutated)	ttctcttttcaaatctaatttcgtttcagagactcccgctataaacgatggattacaaggatgacgac gataaggattacaaggatgacgacgataagggatccgctgacgacgcggcacaggcaggcgaca acgccgaatacatcaagatcaaggtcgttggacaggtaatttg

Table S3 Oligos used for this study

Primer	Description	Sequence
1335	P*U6* primer for site-directed mutagenesis	caagacatctcgcaatagg
1349	sgRNA template sequencing oligo	ctctgacacatgcagctcccgg
1432	Generation of *klp-12* CRISPR/Cas9 plasmid by Q5 mutagensis (pJW1138; pair with oligo 1335)	atccacaagttacaattggGTTTTAGAGCTAGAAATAGCAAGT
1436	*klp-12* genotyping-F	ccatcgaataatccatccacaagtt
1437	*klp-12* genotyping-R	gtttcgcttggggtgtcatgtt
1582	Generation of *nhr-25* CRISPR/Cas9 plasmid by Q5 mutagensis (pJW1185; pair with oligo 1335)	catacactgctgtgccgtacaGTTTTAGAGCTAGAAATAGCAAGT
1584	*nhr-25* C-terminal insert screening-F	agagaagagaagcatcggaag
1586	*nhr-25* C-terminal insert screening-R	tgtgagggtttgggcactagg
1586	*nhr-23* C-terminal insert screening-F	gtgtgcggtgaaaggtattctg
1587	*nhr-23* C-terminal insert screening-R	aatgaggaactctcctgcaac
1715	FLAG-specific oligo for direct screening. Pair with oligo 1585 or 1587.	gggattacaaggatgacgacg
1734	Generation of *nhr-23* CRISPR/Cas9 plasmid by Q5 mutagensis (pJW1254; pair with oligo 1335)	aagagctattcactgcagatGTTTAAGAGCTATGCTGGAAACAG
1763	Generation of *klp-12* CRISPR/Cas9 plasmid by Q5 mutagensis (pJW1236; pair with oligo 1335)	atccacaagttacaattggGTTTAAGAGCTATGCTGGAAACAG
1785	deletion of P*U6*-sgRNA template in pJW1219 to generate pJW1259-F	cgacgttgtaaaacgacggccagt
1786	deletion of P*U6*-sgRNA template in pJW1219 to generate pJW1259-R	ccgggagctgcatgtgtcagagg
1787	P*U6*-F for generating pJW1310 and cloning P*U6* for PCR-derived sgRNA templates	attgtgttcgttgagtgaccc
1788	P*U6*-R for generating pJW1310 and cloning P*U6* for PCR-derived sgRNA templates	caagacatctcgcaataggagg
1789	sgRNA-F for generating pJW1311	gtttaagagctatgctggaaac
1790	sgRNA-R for generating pJW1311 and cloning P*U6*::sgRNA templates	aaaaataggcgtatcacgagg
1793	nested P*U6*-sgRNA template-F	aacgtcgtgactgggaaaacc
1794	nested P*U6*-sgRNA template-R	ggtgtgaaataccgcacagatgc
1827	*nhr-23* PAM #3 P*U6*-sgRNA template by PCR fusion (pair with oligo 1790)	cctcctattgcgagatgtcttGgaagcttttcagatgatgtGTTTAAGAGCTATGCTGGA
1828	*nhr-23* PAM #1 P*U6*-sgRNA template by PCR fusion (pair with oligo 1790)	cctcctattgcgagatgtcttGagagctattcactgcagatGTTTAAGAGCTATGCTGGA
1829	Generation of *nhr-23* PAM#2 CRISPR/Cas9 plasmid by Q5 mutagesis (pJW1268; pair with oligo 1335)	agtgaatagctctttgtagaGTTTAAGAGCTATGCTGGAAACAG
1897	Generation of *pha-1* CRISPR/Cas9 plasmid by Q5 mutagesis (pJW1285; pair with oligo 1335)	atgaataacttgatgaacatGTTTAAGAGCTATGCTGGAAACAG

1898	*pha-1* P*U6*-sgRNA template by PCR fusion (pair with oligo 1790)	cctcctattgcgagatgtcttGatgaataacttgatgaacat GTTTAAGAGCTATGCTGG
1908	*pha-1* genotyping-F	caatttggcagccattcatgtg
1909	*pha-1* genotyping-R	tcgcgcactactgaatcagagtc
1988	*nhr-25* PAM#2 P*U6*-sgRNA template (pair with oligo 1790)	cctcctattgcgagatgtcttGatacactgctgtgccgtaca GTTTAAGAGCTATGCTGG
1995	Generation of *nhr-25* CRISPR/Cas9 plasmid by Q5 mutagensis (pJW1308; pair with oligo 1335)	atacactgctgtgccgtacaGTTTAAGAGCTATGCTG GAAACAG
2093	*nhr-23* sgRNA PAM #4 P*U6*-sgRNA template by PCR fusion (pair with oligo 1790)	cctcctattgcgagatgtcttGatgatgttggatcagacattG TTTAAGAGCTATGCTGG
2097	*lig-4* sgRNA#1 P*U6*-sgRNA template by PCR fusion (pair with oligo 1790)	cctcctattgcgagatgtcttGacgtcttcaacaagattcgg GTTTAAGAGCTATGCTGG
2098	*lig-4* sgRNA#2 P*U6*-sgRNA template by PCR fusion (pair with oligo 1790)	cctcctattgcgagatgtcttGttgacgtcttcaacaagattG TTTAAGAGCTATGCTGG
2104	*smo-1* sgRNA#1 P*U6*-sgRNA template by PCR fusion (pair with oligo 1790); sgRNA is from (KIM *et al.* 2014)	cctcctattgcgagatgtcttGgccgatgatgcagctcaagc GTTTAAGAGCTATGCTGG
2114	*nhr-23* FLAG specific: for sequencing into 5' end of 2xFLAG and 3xFLAG tags in heterozygotes	ttcactgcagatcgacctgg
2115	*nhr-23* FLAG specific: for sequencing into 3' end of 2xFLAG and 3xFLAG tags in heterozygotes	atgatatatggattcagtcact
2117	*nhr-25* FLAG specific: for sequencing into 5' end of 2xFLAG and 3xFLAG tags in heterozygotes	gtaccttatatggcatcagg
2118	*nhr-25* FLAG specific: for sequencing into 3' end of 2xFLAG and 3xFLAG tags in heterozygotes	ctcctatgacagagacattact
2127	*smo-1* genotyping-F	cgctccccagacaatcgata
2128	*smo-1* genotyping-R	tggaaaagggatggatgggtg
2129	*lig-4* genotyping-F	ggcaagactcaagctcggat
2130	*lig-4* genotyping-R	cccatcatccattggtcccg
2135	*smo-1* FLAG specific: for sequencing into 5' end of 2xFLAG tag heterozygotes	ctcccgctataaacgatgga
2136	*smo-1* FLAG specific: for sequencing into 3' end of 2xFLAG tag heterozygotes	gtgccgcgtcgtcagcgg
	GSGGGG-2xFLAG epitope (used in *nhr-23* and *nhr-25* editing)	ggatccggaggtggcggggattacaaggatgacgacgata aggattacaaggatgacgacgataag
	GSGGGG-3xFLAG epitope (used in *nhr-23* and *nhr-25* editing)	ggatccggaggtggcggggactacaaagaccatgacggtg attataaagatcatgatatcgattacaaggatgacgatgaca ag
	2xFLAG-GS epitope (used in *smo-1* editing)	gattacaaggatgacgacgataaggattacaaggatgacga cgataagggatcc

For oligos 1828, 1898, 1988, 2093, 2097, 2098, and 2104, the underlined, lowercase sequence is the sgRNA target site. The uppercase G 1 bp 5' to the sgRNA target is the +1 base of the U6 transcript and the uppercase sequence 3' top the sgRNA target is a portion of the chimeric sgRNA.

For oligos 1432, 1582, 1734, 1763, 1829, 1897, and 1995 the lowercase sequence is the sgRNA target sequence, uppercase sequence is a portion of the chimeric sgRNA .

Table S4 gBlocks used for this study

Primer	Description	Sequence
1643	sgRNA(F+E)	tataaacacctcctattgcgagatgtcttggatggatgtgtagtcaattgtttaagagctatgctggaaacagcatagcaagtt taaataaggctagtccgttatcaacttgaaaaagtggcaccgagtcggtgctttttttgtgaaatttctggcgtaatagcgaa gaggcccgcacc

Table S5 Brood size analysis of indicated genotypes

Strain	Genotype	Broodsize	P0 animals scored	Embryonic lethality (%)	Males (%)	Molting defects (%)
N2	WT	213±45 (n=4465)	19	0.16	0	0 (n=4458)
GE24	*pha-1(e2123)* III	128±34 (n=1520)	12	72.7	0	n/a
KRY42[b]	*nhr-25(kry1[nhr-25::2xFLAG])* X	191±42 (n=3627)	19	1.25	0	0 (n=3627)
KRY71	*pha-1(kry43[Y169C*e2123])* III	210.7±30 (n=2528)	12	1.19	0	0 (n=2528)
KRY49	*nhr-23(kry10[nhr-23::2xFLAG])* I; *pha-1(kry11[Y169C*e2123])* III	167.3±34 (n=1840)	11	1.68	0	0 (n=1840)
KRY64	*pha-1(kry34[Y169C*e2123])* III; *nhr-25(kry35[nhr-25::2xFLAG])* X	146.8±35 (n=1762)	12	2.27	0.11	0 (n=1762)
KRY72	*nhr-23(kry44[nhr-23::3xFLAG])* I; *pha-1(kry45[Y169C*e2123])* III	167.1±68 (n=1671)	10	0.78	0	0 (n=1671)
KRY74	*pha-1(kry48[Y169C*e2123])* III; *nhr-25(kry49[nhr-25::3xFLAG])* X	180.8±48 (n=1671)	12	2.00	0	0 (n=2170)
KRY75	*nhr-23(kry50[nhr-23::3xFLAG])* I;*pha-1(kry51[Y169C*e2123])* III; *nhr-25(kry52[nhr-25::3xFLAG])* X	112.7±46 (n=1352)	12	3.42	0.15	0 (n=1352)

[a]all remaining progeny arrested as larvae.

[b]from direct screening approach. *lig-4(ok716)* removed by outcrossing; strain was outcrossed 6x.

Table S6 Males recovered in injection experiments

P0 strain	Diet	Expt.	*pha-1* oligo	Repair oligo	Viable injected P0	P0 with rescued F1	♂n	♂PCR hit
pha-1(ts)	OP50	Figure 1D	80mer sense	*nhr-23::2xFLAG* sense	16	3	0	0
pha-1(ts)	OP50	Figure 1D	80mer antisense	*nhr-23::2xFLAG* sense	47	3	0	0
pha-1(ts)	OP50	Figure 1D	60mer sense	*nhr-23::2xFLAG* sense	11	3	0	0
pha-1(ts)	OP50	Figure 1D	200mer sense	*nhr-23::2xFLAG* sense	28	10	3	2
pha-1(ts)	OP50	Figure 1D	200mer sense	*nhr-23::2xFLAG* antisense	57	4	0	0
pha-1(ts)	HB101	Figure 3B	200mer sense	*nhr-23::2xFLAG* sense	27	3	0	0
pha-1(ts); control(RNAi)	OP50 then RNAi	Table 2	80mer sense	*nhr-23:::2xFLAG*	10	1	0	0
pha-1(ts); cku-80(RNAi)	OP50 then RNAi	Table 2	80mer sense	*nhr-23:::2xFLAG*	16	6	1	1
pha-1(ts); control(RNAi)	HB101 then RNAi	Table 2	200mer sense	*nhr-25:::2xFLAG*	21	4	1	0
pha-1(ts); cku-80(RNAi)	HB101 then RNAi	Table 2	200mer sense	*nhr-25:::2xFLAG*	22	12	3	0
pha-1(ts); control(RNAi)	HB101 then RNAi	Table 2	200mer sense	*nhr-23::2xFLAG* *nhr-25::3xFLAG*	34	4	0	0 0
pha-1(ts); cku-80(RNAi)	HB101 then RNAi	Table 2	200mer sense	*nhr-23::2xFLAG* *nhr-25::3xFLAG*	13	3	0	0 0
pha-1(ts); cku-80(RNAi)	HB101 then RNAi	Table 2	200mer sense	*2xFLAG::smo-1* *lig-4 stop*	15	7	0	0 0

Table S7 Conversion events associated with different DSB positions for *nhr-23::2xFLAG* knock-ins

sgRNA	DSB Distance from insert site	Sequenced animals	PAM#1 only	PAM#2 only	PAM#3 only	PAM#1+ PAM#2	PAM#2+ PAM#3	PAM#1+ PAM#2+ PAM#3	PAM#1+ FLAG	PAM#1+ PAM#2+ FLAG	PAM#1+ PAM#2+ PAM#3+ FLAG
PAM #1[a]	9 bp	22[b]	n/a	n/a	n/a	n/a	n/a	n/a	16	6	n/a
PAM #2	29 bp	12[c]	0	2	n/a	0	n/a	n/a	0	1	n/a
PAM #3	54 bp	8[d]	0	0	0	0	1	0	0	0	1[e]

For the data presented in Figure 4, the number of animals with conversion events at the indicated PAMs, and number FLAG tag knock-in was presented. Here, a more detailed breakdown of the knock-in events is provided. There was no PAM #3 mutation present in the repair oligo used for the PAM #1 and PAM #2 sgRNA experiments.

[a]Pooled from all 200mer *nhr-23-2xFLAG* injections (Figures 1 and 3, Table 2). As these animals were selected for based on a potential FLAG insertion, there were no "PAM only" gene conversion events that would be identified in this dataset.
[b]Includes 14 precise insertions and 8 partial insertions
[c]Of the 12 sequenced animals, nine had no knocked-in sequence
[d] Of the eight sequenced animals, six had no knocked-in sequence
[e]1 bp deletion in inserted 2xFLAG epitope

Table S8 *nhr-23::2xFLAG* and *nhr-25::2xFLAG* knock-in identification by direct screening

P0 strain	Repair oligo	Oligo polarity	Succesfully injected P0	F1 screened	PCR hits	Precise Knockins	% Knockins per F1	% Knockins per P0
WT	*nhr-25::2xFLAG*	sense	12	380	0	0	0.00	0
lig-4(ok716)	*nhr-25::2xFLAG*	sense	10	768	1	1	0.13	10
WT	*nhr-23::2xFLAG*	sense	2	200	2	0	0	0
lig-4(ok716)	*nhr-23::2xFLAG*	sense	4	800	8	0	0	0

For the *nhr-25* experiments, animals were injected with 100 ng/µl of CRISPR/Cas9 plasmid targeting the same PAM used for the experiments described in Figure 5, 10 ng/µl of a *myo-2::tdTomato* co-injection marker, and 100 ng/µl of a 135mer *nhr-25::2xFLAG* repair oligo with 35 bp homology arms (oligo #1580), which was the synthesis size limit at the time. Injected P0 animals were singly plated, and plates lacking co-injection marker positive F1 progeny were discarded. As Zhao *et al*. (2014) had reported that only non-transgenic F1s contained knock-ins, marker-negative F1 were transferred into 96-well plates (four worms/well), allowed to self-fertilize, and potential knock-ins were identified by PCR and diagnostic *Bam*HI digestion, as in the *pha-1(ts)* co-selection experiments. Oligo polarity is with respect to the coding strand.

For *nhr-23* experiments, animals were injected with 50 ng/µl of a CRISPR/Cas9 plasmid targeting *nhr-23* PAM #1 (Figure 1), 10 ng/µl of a *myo-2::tdTomato* co-injection marker, and 100 ng/µl of a 199mer *2xFLAG* repair oligo with the PAM mutated (oligos #1719). Wells containing marker-positive F1 progeny were identified, all animals from these wells were pooled, and 10 worms were plated per well of a 96-well plate. Following self-fertilization, a portion of the well was taken for genotyping and four rows were pooled for knock-in specific PCR using an oligo internal to the insert and an oligo external to the insert.

Table S9 Summary of strands to which sgRNAs bind, sgRNA activity, repair oligo strand homology, and repair oligo efficiency

Gene	sgRNA sequence[a]	Strand to which sgRNA binds[b]	sgRNA activity	Repair oligo	Repair oligo strand[c]	Repair oligo efficiency
pha-1(e2123)	atgaataacttgatga acat(cgg)	coding	Y	60, 80 and 200 mer *pha-1(ts)* repair (oligos 1899, 1986, 1987)	coding	High
				80mer *pha-1(ts)* repair (oligo 1985)	template	Weak
nhr-23 PAM #1	agagctattcactgcagat(cgg)	template	Y	200mer *nhr-23::2xFLAG* (oligo 1831, 2 PAMs mut)	coding	High
				200mer *nhr-23::2xFLAG* (oligo 1832, 2 PAMs mut)	template	Weak
				193mer *nhr-23::3xFLAG* (oligos 2015 and 2085, 2 PAMs mut)	coding	Moderate
nhr-23 PAM #2	agtgaatagctctttgtaga(ggg)	coding	Y	200mer *nhr-23::2xFLAG* (oligo 1831, 2 PAMs mut)	template	Moderate
nhr-23 PAM #3	ggaagcttttcagatgatgt(tgg)	coding	Y (moderate)	200mer *nhr-23::2xFLAG* (oligo 2089, 3 PAMs mut)	template	Moderate
nhr-23 PAM #4	atgatgttggatcagacatt(cgg)	coding	N	200mer *nhr-23::2xFLAG* (oligo 2089, 3 PAMs mut)	template	n/a (sgRNA fail)
nhr-25	atacactgctgtgccgtaca(tgg)	template	Y	175mer *nhr-25::2xFLAG* (oligo 1989; PAM mut)	template	Moderate
				193mer *nhr-25::3xFLAG* (oligo 2014; PAM mut)-unpurified	template	Weak
				193mer *nhr-25::3xFLAG* (oligo 2085; PAM mut)-PAGE purified	template	Weak
smo-1	gccgatgatgcagctcaagc(agg)	template	Y	175mer *2xFLAG::smo-1* (oligo 2105; PAM mutated)	template	High
lig-4	acgtcttcaacaagattcgg(cgg)	template	N	60mer *lig-4* stop/exon deletion (oligo 2099)	template	n/a (sgRNA fail)
	ttgacgtcttcaacaagatt(cgg)	template	N			

[a]sgRNA target sequence. The PAM sequence is provided in brackets.
[b]strand to which sgRNA binds. ie. for a target sequence with an "NGG" PAM in the coding sequence, the sgRNA would bind to the template strand
[c]strand from which oligo homology is derived

Supplemental references

FRIEDLAND A. E., TZUR Y. B., ESVELT K. M., COLAIÁCOVO M. P., CHURCH G. M., CALARCO J. A., 2013 Heritable genome editing in *C. elegans* via a CRISPR-Cas9 system. Nat Meth **10**: 741–743.

KIM H., ISHIDATE T., GHANTA K. S., SETH M., CONTE D., SHIRAYAMA M., MELLO C. C., 2014 A Co-CRISPR Strategy for Efficient Genome Editing in *Caenorhabditis elegans*. Genetics **197**: 1069–1080.

ZHAO P., ZHANG Z., KE H., YUE Y., XUE D., 2014 Oligonucleotide-based targeted gene editing in *C. elegans* via the CRISPR/Cas9 system. Cell Research **24**: 247–250.